Mechanics of Materials 93 (2016) 168–183

Contents lists available at ScienceDirect

Mechanics of Materials

journal homepage: www.elsevier.com/locate/mechmat

Dispersion relations of elastic waves in one-dimensional piezoelectric phononic crystal with mechanically and dielectrically imperfect interfaces

Xiao Guo [a], Peijun Wei [a,b,*], Li Li [a]

[a] Department of applied mechanics, University of Science and Technology Beijing, Beijing 100083, China
[b] State Key Laboratory of Nonlinear Mechanics (LNM), Chinese Academy of Science, Beijing, Beijing 100080, China

ARTICLE INFO

Article history:
Received 3 June 2015
Revised 21 September 2015
Available online 14 November 2015

Keywords:
Dispersion relations
Piezoelectricity
Phononic crystal
Imperfect interface
Bloch wave
Transfer matrix

ABSTRACT

The effects of mechanically and dielectrically imperfect interfaces on dispersion relations of elastic waves in a one-dimensional piezoelectric phononic crystal are studied in this paper. Six kinds of imperfect interfaces between two different piezoelectric materials constituting the phononic crystal are considered. These imperfect interfaces include: the mechanically compliant dielectrically weakly conducting interface, the mechanically compliant dielectrically highly conducting interface, the grounded metallized interface, the low dielectric interface, the tangent fixed interface and the tangent slippery interface. Based on transfer matrices of piezoelectric slabs and imperfect interfaces, the total transfer matrix of a typical single cell in the periodical structure is obtained. Furthermore, the Bloch theorem is used to obtain the dispersive equations of in-plane and anti-plane Bloch waves. The dispersive equations are solved numerically and the numerical results are shown graphically. In the case of normal propagation of elastic waves within piezoelectric slabs, the analytical expressions of the dispersion equations are derived and compared with other literatures. The influences of mechanically and dielectrically imperfect interfaces on the dispersive relations are discussed based on the numerical results.

1. Introduction

As a kind of artificial periodic composite materials or structures, phononic crystal can give rise to complete acoustic band gaps within which elastic waves propagation are forbidden while in other frequency ranges elastic waves can propagate without exhaustion. Therefore, phononic crystal can be used to control the propagation of elastic waves and thus attracted attentions of many researcher, such as, Sigalas and Economou (1992), Kushwaha et al. (1993), Kafesaki et al. (1995), Suzuki and Yu (1998), and Liu et al. (2000). In recent years, piezoelectric materials were introduced into the manufacture of phononic crystal due to its unique electromechanical coupling effect. Alvarez-Mesquida et al (2001) studied the shear horizontal wave propagation processes in a layered piezoelectric composite based on a recursive system of equations involving the piezoelectric impedance. Qian (2004a, 2004b) studied the propagation behavior of horizontally polarized shear waves (SH-waves) in a periodic piezoelectric-polymeric layered structure. The dispersive equation and the phase velocity of SH-waves were obtained. Further, the influence of initial stress on the stop band and the dispersion relation of the SH-waves was discussed in detail. Monsivais et al. (2005) studied surface and shear horizontal waves in finite and infinite piezoelectric composite media, considering the transmission, dispersion relation, angular dispersion relation, and eigenmodes of vibration of the

* Corresponding author at: Department of applied mechanics, University of Science and Technology Beijing, Beijing 100083, China. Tel./fax: +86 10 82388981.
E-mail address: weipj@ustb.edu.cn (P. Wei).

http://dx.doi.org/10.1016/j.mechmat.2015.11.004
0167-6636/

composites. Chen and Wang (2007) studied the band gaps of both in-plane and anti-plane elastic waves propagating along an arbitrary direction in one-dimensional disordered phononic crystals. The localization of wave propagation due to random disorder was discussed by introducing the concept of the localization factor. It is found that phononic quasicrystals involve more bands with localization of wave motion compared with the periodic structure. The localization factor may act as an accurate and efficient parameter to characterize band structures of both ordered and disordered (including quasi-periodic) phononic crystals. Pang et al. (2008, 2014) studied the wave propagation in layered periodic composites consisting of piezoelectric and piezomagnetic phases and derived the dispersion relations of Lamb waves and SH waves. Wang et al. (2008, 2010) investigated the elastic wave propagation in two-dimensional and three-dimensional phononic crystals with piezoelectric and piezomagnetic inclusions taking the magneto-electro-elastic coupling or initial stress into account.

However, the investigations above mentioned are based on the perfect interface, namely, all mechanical and dielectric quantities, for example, the displacement components, the traction components, the electric potential and the electrical displacement components, are assumed to be continuous across the interface. In actual situation, the appearances of imperfect interfaces due to the accumulative interfacial damages, local debonding or manufacturing defection is always inevitable. The influences of imperfect interfaces on the dispersive relations and the band gaps of the phononic crystal are therefore interesting. Fan et al. (2006) investigated certain waves which created the fluctuation perpendicular to the incident plane and propagated near an imperfectly bonded interface between two half-spaces of different piezoelectric materials. The existence of these waves relies on the imperfection of the interface bonding. Huang et al (2009) studied the interfacial SH waves propagating along the imperfectly bonded interface of a magnetoelectric composite consisting of piezoelectric (PE) and piezomagnetic (PM) phases. It was shown that the interfacial imperfection strongly affects the velocity of interfacial shear waves and the interfacial shear waves do not exist for the perfect interface. Zheng and Wei (2009) investigated the dispersive relations and the band gaps of elastic waves in 1-D phononic crystals. In their study, the imperfect interface with the traction components jumps or the displacement components jumps was considered. Pang and Liu (2011) investigated the reflection and transmission of plane waves at an interface between piezoelectric (PE) and piezomagnetic (PM) media. The mechanical imperfection of bonding behavior at the interface was described as the linear spring model. But dielectrically imperfect interfaces were not considered. Lan and Wei (2012, 2014) studied the influence of the imperfect interface on the dispersive characteristics and the band gaps of SH waves propagating through laminated piezoelectric phononic crystal. The imperfect interface is modeled as a thin membrane with elasticity and inertial even but without thickness or a thin interlayer with gradient variation of material parameters. However, the imperfect interface involved in their investigations is merely mechanically imperfect. The interface with dielectrically imperfect is not considered. In fact, the dielectric quantities may also be discontinuous across the interface. Sun et al (2011) studied the propagation of SH wave in a cylindrically multiferroic composite consisting of a piezoelectric layer and a piezomagnetic central cylinder in which the interface was damaged mechanically, magnetically or electrically. Piliposyan (2012) investigated the existence and propagation of a surface SH wave at the interface of two magneto-electro-elastic half-spaces. Four sets of boundary conditions, namely, full contact, partial contact with magnetically closed boundaries, partial contact with electrically closed boundaries and no electromagnetic contact, were considered. Alshits and Shuvalov (1993, 1995) once studied the reflection problem of transverse elastic waves from a periodic structure of piezomagnetic layers with thin superconducting interlayers and also from a periodic structure of piezoelectric layers with metallized interface. It was shown that the reflection coefficient can jump abruptly from zero to values close to unity when the phase state of the superconducting interlayers changes, which could be caused by a temperature change or an electric current. Wang and Sudak (2007) studied the influence of the mechanically compliant and dielectrically weakly (or highly) conducting interface when presented the analytical solution of a piezoelectric screw dislocation located within one of two joined piezoelectric half-planes. For the mechanically compliant interface, displacements are discontinuous across the interface. Similarly, the electric potential is discontinuous for the dielectrically weakly conducting interface and the normal component of electric displacement is discontinuous for the dielectrically highly conducting interface.

In this paper, the one-dimensional phononic crystal composed of two different piezoelectric materials with the mechanically and dielectrically imperfect interfaces are both considered. First, the transfer matrices of piezoelectric slabs and imperfect interfaces are derived from the motion equation of piezoelectric solids and mechanically and dielectrically interface conditions. Then, the total transfer matrix of one typical single cell of the periodical structure is obtained by the combination of the transfer matrices of piezoelectric slabs and that of imperfect interfaces. Finally, the Bloch theorem is used to obtain the dispersive equations of Bloch waves. Six kinds of imperfect interfaces between two different piezoelectric slabs are considered. These imperfect interfaces include: the mechanically compliant dielectrically weakly conducting interface, the mechanically compliant dielectrically highly conducting interface, the grounded metallized interface, the low dielectric interface, the tangent fixed interface and the tangent slippery interface. The dispersion equations of in-plane Bloch wave and anti-plane Bloch wave are both solved to obtain the dispersive curves and the numerical results are shown graphically. Based on these numerical results, influences of mechanically and dielectrically imperfect interfaces on the dispersive curves are discussed. Moreover, the analytical expressions of the dispersion equation are derived for the normal propagation situation of elastic waves within piezoelectric slabs and are compared with other literatures.

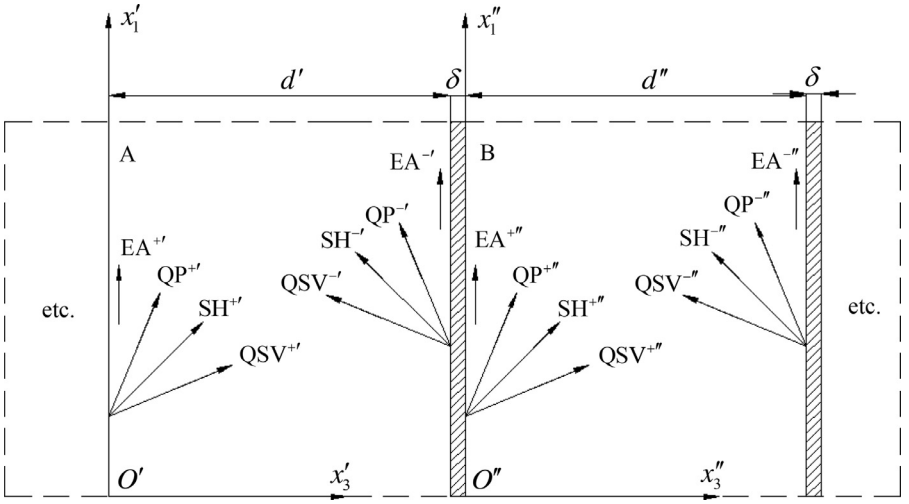

Fig. 1. One-dimensional piezoelectric phononic crystal with imperfect interfaces.

2. Transfer matrix of coupled waves in a slab

Consider a one-dimensional phononic crystal which is formed by periodically repeating two different transversely isotropic piezoelectric slabs. The two different piezoelectric slabs are bonded together but the connection status is not perfect mechanically or dielectrically, and is modeled as the imperfect interface, which means that the mechanical or dielectric quantities may be discontinuous across the interface. Let the x_3-axis is the poling direction and the slab is transversely isotropic in the ox_1x_2 coordinates plane. The physical parameters of slab A and slab B are labeled with the superscript "′" and "″", respectively. In latter formulation, if the physical quantity does not have any superscript, it will be appropriate for these two slabs. C_{ijmn}, e_{mij} and ε_{mi} are the elastic, piezoelectric and dielectric parameters, respectively. ρ and d are the mass density and thickness. There are forward and backward QP (quasi-longitudinal) waves, QSV (quasi-transverse) waves and SH (shear-horizonal) waves in each slab, see Fig. 1. The EA (electro-acoustic) wave always propagates along the interface.

The constitutive equation of transversely isotropic piezoelectric material is (Auld, 1990)

$$\begin{Bmatrix}\sigma_{11}\\ \sigma_{22}\\ \sigma_{33}\\ \sigma_{23}\\ \sigma_{31}\\ \sigma_{12}\end{Bmatrix} = \begin{bmatrix} C_{11} & C_{12} & C_{13} & 0 & 0 & 0\\ C_{12} & C_{11} & C_{13} & 0 & 0 & 0\\ C_{13} & C_{13} & C_{33} & 0 & 0 & 0\\ 0 & 0 & 0 & C_{44} & 0 & 0\\ 0 & 0 & 0 & 0 & C_{44} & 0\\ 0 & 0 & 0 & 0 & 0 & C_{66}\end{bmatrix} \cdot \begin{Bmatrix}S_{11}\\ S_{22}\\ S_{33}\\ 2S_{23}\\ 2S_{31}\\ 2S_{12}\end{Bmatrix} - \begin{bmatrix} 0 & 0 & e_{31}\\ 0 & 0 & e_{31}\\ 0 & 0 & e_{33}\\ 0 & e_{15} & 0\\ e_{15} & 0 & 0\\ 0 & 0 & 0\end{bmatrix} \cdot \begin{Bmatrix}E_1\\ E_2\\ E_3\end{Bmatrix} \tag{1a}$$

$$\begin{Bmatrix}D_1\\ D_2\\ D_3\end{Bmatrix} = \begin{bmatrix} 0 & 0 & 0 & 0 & e_{15} & 0\\ 0 & 0 & 0 & e_{15} & 0 & 0\\ e_{31} & e_{31} & e_{33} & 0 & 0 & 0\end{bmatrix} \cdot \begin{Bmatrix}S_{11}\\ S_{22}\\ S_{33}\\ 2S_{23}\\ 2S_{31}\\ 2S_{12}\end{Bmatrix} + \begin{bmatrix} \varepsilon_{11} & 0 & 0\\ 0 & \varepsilon_{11} & 0\\ 0 & 0 & \varepsilon_{33}\end{bmatrix} \cdot \begin{Bmatrix}E_1\\ E_2\\ E_3\end{Bmatrix} \tag{1b}$$

where $C_{66} = 0.5(C_{11} - C_{12})$. σ_{ij} and S_{mn} are the stress and strain tensor, respectively. E_m and D_m are the electric field and electric displacement vector, respectively. The strain tensor S_{mn} is related with the displacement u_n by $S_{mn} = 0.5(u_{n,m} + u_{m,n})$ while the electric field E_m is related with the electric potential φ by

$$E_m = -\varphi_{,m} \tag{2}$$

in the quasi static electric field approximation.

The mechanical and electrical governing equation can be expressed as

$$\begin{cases}\sigma_{ij,i} = \rho\ddot{u}_j\\ D_{m,m} = 0\end{cases} \tag{3}$$

In either plane strain or anti-plane strain case, the displacement and the electric potential are only the function of x_1 and x_3 which can be assumed as

$$\{u_1, u_2, u_3, \varphi\} = \{U_1, U_2, U_3, \Phi\} \exp\left[\mathbf{i}k_1(x_1 + \xi x_3 - ct)\right] \tag{4}$$

where the wavenumber $\mathbf{k} = (k_1, k_2, k_3) = (k_1, 0, k_3)$ and k_1 is the component of the wave vector along the interface. $\xi(= k_3/k_1)$ is the ratio of wave number and is related with the propagation direction angle by $\theta = \mathbf{arccot}\xi$. ω is the angular frequency. $c(= \omega/k_1)$ is the ratio of the angular frequency with respect to the projection of wave vector along the interface.

Inserting Eqs. (1), (2) and (4) into Eq. (3) leads to

$$k_1^2 \begin{bmatrix} W_{11} & 0 & W_{13} & W_{14}\\ 0 & W_{22} & 0 & 0\\ W_{31} & 0 & W_{33} & W_{34}\\ W_{41} & 0 & W_{43} & W_{44}\end{bmatrix} \cdot \begin{Bmatrix}U_1\\ U_2\\ U_3\\ \Phi\end{Bmatrix} = \begin{Bmatrix}0\\ 0\\ 0\\ 0\end{Bmatrix} \tag{5}$$

It is noticed from Eq. (5) that the electric potential φ is only coupled with the displacement components u_1 and u_3. Therefore, SH wave is independent of the dielectric parameters of slab and the dielectrically interface conditions. The explicit expressions of W_{ij} for the traverse isotropic piezoelectric solid are given in Appendix A.

If we select the isotropic plane ox_1x_2 as the propagation plane of in-plane elastic waves and the poling direction of piezoelectric materials is perpendicular to the normal of interface, Eq. (4) should be modified as

$$\{u_1, u_2, u_3, \varphi\} = \{U_1, U_2, U_3, \Phi\} \exp\left[\mathbf{i}k_1(x_1 + \xi x_2 - ct)\right] \tag{6}$$

where the wavenumber $\mathbf{k} = (k_1, k_2, k_3) = (k_1, k_2, 0)$ and the ratio of wave number $\xi = k_2/k_1$. As a result of this situation, Eq. (5) becomes

$$k_1^2 \begin{bmatrix} \hat{W}_{11} & \hat{W}_{12} & 0 & 0 \\ \hat{W}_{21} & \hat{W}_{22} & 0 & 0 \\ 0 & 0 & \hat{W}_{33} & \hat{W}_{34} \\ 0 & 0 & \hat{W}_{43} & \hat{W}_{44} \end{bmatrix} \cdot \begin{Bmatrix} U_1 \\ U_2 \\ U_3 \\ \Phi \end{Bmatrix} = \begin{Bmatrix} 0 \\ 0 \\ 0 \\ 0 \end{Bmatrix}. \tag{7}$$

The explicit expressions of $\hat{W}_{ij}$ are also given in Appendix A. Instead of the displacement components u_1 and u_2, the electric potential φ is now coupled with the displacement component u_3, as is shown in Eq. (7).

The condition of existing non-trivial solution of Eq. (5) is

$$\begin{vmatrix} W_{11} & W_{13} & W_{14} \\ W_{31} & W_{33} & W_{34} \\ W_{41} & W_{43} & W_{44} \end{vmatrix} = f_1(\xi, c) = 0 \tag{8a}$$

$$W_{22} = f_2(\xi, c) = 0 \tag{8b}$$

For a given c, $f_1(\xi, c)$ is a polynomial of three orders about ξ^2, thus there are three pairs of roots about ξ. Similarly, there are one pairs of roots from equation $f_2(\xi, c) = 0$. These roots stand for all possible wave modes in the piezoelectric solid. The real roots stand for the bulk waves propagating in the ox_1x_3 plane. The imaginary roots stand for the surface waves propagating along interface with attenuation vertical to the propagation direction. The complex roots stands for the bulk wave accompanied with attenuation. For the traverse isotropic solids considered, the value of ξ indicates that there are eight possible part waves. Six of them are bulk waves and two of them are the surface wave. Let ξ_1, ξ_3, ξ_5 and ξ_7 are the forward QP, QSV, SH, EA waves, while ξ_2, ξ_4, ξ_6 and ξ_8 are the backward QP, QSV, SH and EA waves.

Define the amplitude ratio in each coupled wave

$$\begin{cases} G_3 = \frac{U_3}{U_1} = \frac{W_{14}W_{31} - W_{11}W_{34}}{W_{13}W_{34} - W_{14}W_{33}} \\ G_\varphi = \frac{\Phi}{U_1} = \frac{W_{11}W_{33} - W_{13}W_{31}}{W_{13}W_{34} - W_{14}W_{33}} \end{cases} \tag{9}$$

then, $(1, G_3, G_\varphi)$ stands for the coupled relation between the displacement components u_1, u_3 and the electric potential φ. $(1, G_3, G_\varphi)$ can be called the vibration mode. For the coupled waves, namely, QP, QSV and EA waves, the displacement components and the electric potential can be expresses as

$$\begin{aligned} &\{u_{1q}, u_{2q}, u_{3q}, \varphi_q\} \\ &\quad = \{1, 0, G_{3q}, G_{\varphi q}\} U_{1q} \exp\left[\mathbf{i}k_1\left(x_1 + \xi_q x_3 - ct\right)\right] \end{aligned} \tag{10}$$

where the subscript q denotes different types of coupled waves. It is noticed that the well-known Snell's law, namely, k_1, c and ω are same for various coupled waves, is assumed in Eq. (10). Inserting Eq. (10) into Eq. (1), the traction components and the electric displacement components can be expressed as

$$\begin{aligned} &\{\sigma_{33q}, \sigma_{23q}, \sigma_{31q}, D_{3q}\} \\ &\quad = \mathbf{i}k_1 \{H_{3q}, 0, H_{1q}, J_q\} U_{1q} \exp\left[\mathbf{i}k_1\left(x_1 + \xi_q x_3 - ct\right)\right] \end{aligned} \tag{11}$$

where $H_{3q} = C_{13} + C_{33}G_{3q}\xi_q + e_{33}G_{\varphi q}\xi_q$, $H_{1q} = C_{44}(\xi_q + G_{3q}) + e_{15}G_{\varphi q}$, $J_q = e_{31} + e_{33}G_{3q}\xi_q - \varepsilon_{33}G_{\varphi q}\xi_q$.

For SH wave, Eqs. (10)–(11) are replaced by

$$\begin{aligned} &\{u_{1q}, u_{2q}, u_{3q}, \varphi_q\} \\ &\quad = \{0, 1, 0, 0\} U_{2q} \exp\left[\mathbf{i}k_1\left(x_1 + \xi_q x_3 - ct\right)\right] \end{aligned} \tag{12}$$

$$\begin{aligned} &\{\sigma_{33q}, \sigma_{23q}, \sigma_{31q}, D_{3q}\} \\ &\quad = \mathbf{i}k_1 \{0, C_{44}\xi_q, 0, 0\} U_{2q} \exp\left[\mathbf{i}k_1\left(x_1 + \xi_q x_3 - ct\right)\right] \end{aligned} \tag{13}$$

In the normal propagation situation ($k_1 = 0$ or $c = \infty$), there are

$$\begin{aligned} &\{u_{3q}, \varphi_q, \sigma_{33q}, D_{3q}\} = \left\{1, e_{33}/\varepsilon_{33}, \mathbf{i}k_{3q}\left[C_{33} + \left(e_{33}^2/\varepsilon_{33}\right)\right], 0\right\} \\ &\quad U_{3q} \exp\left[\mathbf{i}(k_{3q}x_3 - \omega t)\right] \end{aligned} \tag{14a}$$

where $k_{31} = -k_{32} = \omega\sqrt{\rho/[C_{33} + (e_{33}^2/\varepsilon_{33})]}$, $q = 1,2$ stands for forward and backward P wave, respectively.

$$\{u_{1q}, \sigma_{31q}\} = \{1, \mathbf{i}k_{3q}C_{44}\} U_{1q} \exp\left[\mathbf{i}(k_{3q}x_3 - \omega t)\right] \tag{14b}$$

where $k_{33} = -k_{34} = \omega\sqrt{\rho/C_{44}}$, $q = 3,4$ stands for forward and backward SV wave, respectively.

$$\{u_{2q}, \sigma_{23q}\} = \{1, \mathbf{i}k_{3q}C_{44}\} U_{2q} \exp\left[\mathbf{i}(k_{3q}x_3 - \omega t)\right] \tag{14c}$$

where $k_{35} = -k_{36} = \omega\sqrt{\rho/C_{44}}$, $q = 5,6$ stands for forward and backward SH wave, respectively.

$$\begin{aligned} &\{u_{3q}, \varphi_q, \sigma_{33q}, D_{3q}\} \\ &\quad = \{0, 1 + k_{3q}x_3, e_{33}k_{3q}, -\varepsilon_{33}k_{3q}\} \Phi_q \exp(-\mathbf{i}\omega t) \end{aligned} \tag{14d}$$

where $k_{37} = -k_{38} = 1$, $q = 7,8$ stands for forward and backward EA wave, respectively.

It is noticed from Eq. (14) that QSV and QP waves in the oblique propagation situation reduce to SV wave and P wave in the normal propagation situation. In other word, the polarized displacement directions of the shear vertical and the shear horizontal waves are perpendicular to the wave vector while the polarized displacement direction of dilatational wave is coincident with the wave vector. Besides, SV wave and SH wave are both decoupled with the electric potential φ while P wave is coupled to the electric potential φ. EA wave actually become into a standing wave constrained in a slab in the normal propagation situation. The wave speed of SV, SH and P waves are, respectively,

$$\begin{cases} c_{\mathrm{P}} = \sqrt{\left[C_{33} + \left(e_{33}^2/\varepsilon_{33}\right)\right]/\rho} \\ c_{\mathrm{SV}} = c_{\mathrm{SH}} = \sqrt{C_{44}/\rho} \end{cases} \tag{15}$$

For convenience of the statement of the interface conditions and the periodic condition, we define the state vector of the mechanical and the dielectric fields as

$$\mathbf{V}(x_i, t) = \left\{\bar{u}_1, \bar{u}_3, \bar{\varphi}, \bar{\sigma}_{33}, \bar{\sigma}_{31}, \bar{D}_3\right\}^T \tag{16a}$$

for in-plane Bloch wave and

$$\mathbf{V}(x_i,t)=\{\bar{u}_2,\bar{\sigma}_{23}\}^T \tag{16b}$$

for anti-plane Bloch wave, where $\bar{u}_1=\sum_{q=1,2.3}^{4,7,8}u_{1q}$, $\bar{u}_2=\sum_{q=5}^{6}u_{2q}$, $\bar{u}_3=\sum_{q=1,2,3}^{4,7,8}u_{3q}$, $\bar{\varphi}=\sum_{q=1,2,3}^{4,7,8}\varphi_q$, $\bar{\sigma}_{33}=\sum_{q=1,2,3}^{4,7,8}\sigma_{33q}$, $\bar{\sigma}_{23}=\sum_{q=5}^{6}\sigma_{23q}$, $\bar{\sigma}_{31}=\sum_{q=1,2,3}^{4,7,8}\sigma_{31q}$, $\bar{D}_3=\sum_{q=1,2,3}^{4,7,8}D_{3q}$.

For in-plane Bloch wave, the state vectors at the left and at the right boundaries of a slab can be expressed as

$$\mathbf{V}_L(x_3=0^+,t)=\mathbf{T}_L\{U_{11},U_{12},U_{13},U_{14},U_{17},U_{18}\}^T\exp[\mathbf{i}k_1(x_1-ct)] \tag{17a}$$

$$\mathbf{V}_R(x_3=d^-,t)=\mathbf{T}_R\{U_{11},U_{12},U_{13},U_{14},U_{17},U_{18}\}^T\exp[\mathbf{i}k_1(x_1-ct)] \tag{17b}$$

Similarly, for anti-plane Bloch wave,

$$\mathbf{V}_L(x_3=0^+,t)=\mathbf{T}_L\{U_{25},U_{26}\}^T\exp[\mathbf{i}k_1(x_1-ct)] \tag{18a}$$

$$\mathbf{V}_R(x_3=d^-,t)=\mathbf{T}_R\{U_{25},U_{26}\}^T\exp[\mathbf{i}k_1(x_1-ct)] \tag{18b}$$

The state vectors at the left and at the right boundaries of a slab can be related by

$$\mathbf{V}_R(x_3=d^-,t)=\mathbf{T}\mathbf{V}_L(x_3=0^+,t) \tag{19}$$

where $\mathbf{T}=\mathbf{T}_R\mathbf{T}_L^{-1}$ is the transfer matrices of the slab. It is noted that the transfer matrix $\mathbf{T}$ is of 6×6 order for in-plane Bloch wave and 2×2 order for anti-plane Bloch wave. The explicit expressions of T_L and T_R are given in appendix B.

In the case of normal propagation, we can define the state vector as

$$\mathbf{V}(x_3,t)=\left\{\bar{u}_3,\bar{\varphi},\bar{\sigma}_{33},\bar{D}_3\right\}^T \tag{20a}$$

for Bloch P wave.

$$\mathbf{V}(x_3,t)=\{\bar{u}_1,\bar{\sigma}_{31}\}^T \tag{20b}$$

for Bloch SV wave, and

$$\mathbf{V}(x_3,t)=\{\bar{u}_2,\bar{\sigma}_{23}\}^T \tag{20c}$$

for Bloch SH wave. The state vectors at the left and at the right boundaries of a slab can still be related by the transfer matrix, namely, Eq. (19). But the transfer matrix $\mathbf{T}$ is of 4×4 order for Bloch P wave and 2×2 order for Bloch SV and SH waves.

3. Transfer matrix of a single cell with imperfect interfaces

3.1. Mechanically compliant, dielectrically weakly and highly conducting imperfect interface

For the perfect interface, all mechanical and dielectric fields, for example, the displacement components, the traction components, the electric potential and the normal component of electric displacement, are continuous across the interface. In other words, the state vectors at two sides of the interface are same. Accordingly, the transfer matrix of the perfect interface is a unit matrix. For the imperfect interface, parts of mechanical or dielectric fields are not continuous. Physically, the imperfect interface is a result of approximating the thin interlayer (with a finite thickness although very thin) between two dissimilar piezoelectric solids with a mathematic interface without thickness. The state vectors at two sides of the imperfect interface are not the same any more. By the introduction of the transfer matrix of the imperfect interface, the state vectors at two sides of the imperfect interface can be related by

$$\begin{cases}\mathbf{V}'_L(x_3=0^+,t)=\mathbf{T}_\delta\mathbf{V}''_R\left(x_3=d''^-,t\right)\\ \mathbf{V}''_L(x_3=0^+,t)=\mathbf{T}_\delta\mathbf{V}'_R\left(x_3=d'^-,t\right)\end{cases} \tag{21}$$

where $\mathbf{T}_\delta$ denotes the transfer matrix of the imperfect interface. For different types of imperfect interfaces, the transfer matrix $\mathbf{T}_\delta$ may have different expressions.

For the mechanically compliant, dielectrically weakly conducting interface, the interface conditions are expressed as (Wang and Sudak, 2007)

$$\begin{aligned}&\bar{u}_1''-\bar{u}_1'=\alpha\bar{\sigma}_{31}',\ \bar{u}_2''-\bar{u}_2'=\beta\bar{\sigma}_{23}',\ \bar{u}_3''-\bar{u}_3'=\gamma\bar{\sigma}_{33}',\\ &\bar{\varphi}''-\bar{\varphi}'=-\eta\bar{D}_3',\ \bar{\sigma}_{3i}''=\bar{\sigma}_{3i}',\ \bar{D}_3''=\bar{D}_3',\ (i=1,2,3)\end{aligned} \tag{22a}$$

For the mechanically compliant, dielectrically highly conducting interface, the interface conditions can be expressed as (Wang and Sudak, 2007)

$$\begin{aligned}&\bar{u}_1''-\bar{u}_1'=\alpha\bar{\sigma}_{31}',\ \bar{u}_2''-\bar{u}_2'=\beta\bar{\sigma}_{23}',\ \bar{u}_3''-\bar{u}_3'=\gamma\bar{\sigma}_{33}',\\ &\bar{\varphi}''=\bar{\varphi}',\ \bar{\sigma}_{3i}''=\bar{\sigma}_{3i}',\ \bar{D}_3''-\bar{D}_3'=\chi\frac{\partial^2\bar{\varphi}'}{\partial x_1^2},\ (i=1,2,3)\end{aligned} \tag{22b}$$

The parameter α, β and γ in Eq. (22) represent the imperfectly mechanical propertied of interfaces and the parameter η and χ the imperfectly dielectric properties of interfaces. When all parameters in Eq. (22) are equal to zero, these two types of imperfect interfaces reduce to perfect interfaces. If $\alpha,\beta,\gamma\to\infty$, it leads to $\bar{\sigma}_{31},\bar{\sigma}_{23},\bar{\sigma}_{33}\to0$ and thus Eq. (22) describes completely debonded interfaces. If $\eta\to\infty$, it leads to $\bar{D}_3\to0$ and thus Eq. (22a) describes a charge-free interface. So a finite value of η describes the dielectrically weakly conducting property of the imperfect interface. If $\chi\to\infty$, it leads to $\bar{\varphi}\to0$ and thus Eq. (22b) describes a equipotential grounded interface. So a finite value of η describes the dielectrically highly conducting property of the imperfect interface.

In the case of in-plane Bloch wave, the interface transfer matrix can be expressed as

$$\mathbf{T}_{\delta(in)}=\begin{bmatrix}1&0&0&0&\alpha&0\\0&1&0&\gamma&0&0\\0&0&1&0&0&-\eta\\0&0&0&1&0&0\\0&0&0&0&1&0\\0&0&0&0&0&1\end{bmatrix} \tag{23a}$$

for the mechanically compliant, dielectrically weakly conducting interface and

$$\mathbf{T}_{\delta(in)} = \begin{bmatrix} 1 & 0 & 0 & 0 & \alpha & 0 \\ 0 & 1 & 0 & \gamma & 0 & 0 \\ 0 & 0 & 1 & 0 & 0 & 0 \\ 0 & 0 & 0 & 1 & 0 & 0 \\ 0 & 0 & 0 & 0 & 1 & 0 \\ 0 & 0 & -k_1^2\chi & 0 & 0 & 1 \end{bmatrix} \tag{23b}$$

for the mechanically compliant, dielectrically highly conducting interface. In the case of anti-plane Bloch wave, the electric potential is decoupled with the displacement component u_2. Therefore, the dielectrically imperfect interface has no any influence on the SH wave propagation and only the mechanically compliant imperfect interface influence anti-plane Bloch wave propagation. In this situation,

$$\mathbf{T}_{\delta(anti)} = \begin{bmatrix} 1 & \beta \\ 0 & 1 \end{bmatrix} \tag{24}$$

In the case of normal propagation, the transfer matrices $\mathbf{T}_\delta$ of imperfect interfaces reduces to

$$\mathbf{T}_{\delta(\mathrm{P})} = \begin{bmatrix} 1 & 0 & \gamma & 0 \\ 0 & 1 & 0 & -\eta \\ 0 & 0 & 1 & 0 \\ 0 & 0 & 0 & 1 \end{bmatrix}, \mathbf{T}_{\delta(\mathrm{SV})} = \begin{bmatrix} 1 & \alpha \\ 0 & 1 \end{bmatrix}, \mathbf{T}_{\delta(\mathrm{SH})} = \begin{bmatrix} 1 & \beta \\ 0 & 1 \end{bmatrix}. \tag{25}$$

The dielectrically highly conducting imperfect interface does not have any influence on the dispersion relations of Bloch P wave.

For a single cell composed of slab A and slab B and imperfect interfaces between them, the state vectors at the left and right boundaries are related by

$$\mathbf{V}'_L\left[x_3 = \left(d' + d''\right)^+, t\right] = \mathbf{T}_\delta \mathbf{T}'' \mathbf{T}_\delta \mathbf{T}' \mathbf{V}'_L(x_3 = 0^+, t) \tag{26}$$

Therefore, the transfer matrices of a typical single cell can be expressed as

$$\mathbf{T}_{\mathrm{cell}} = \mathbf{T}_\delta \mathbf{T}'' \mathbf{T}_\delta \mathbf{T}' \tag{27}$$

where $\mathbf{T}'$ and $\mathbf{T}''$ are the transfer matrices of slab A and slab B, respectively.

3.2. Low dielectric interface and grounded metallized interface

The interface conditions of the low dielectric interface can be expressed as (Alshits and Shuvalov, 1993)

$$\bar{u}'_i = \bar{u}''_i, \bar{\sigma}'_{3i} = \bar{\sigma}''_{3i}, \bar{D}'_3 = \bar{D}''_3 = 0, (i = 1, 3). \tag{28}$$

It can be taken for the limiting case when the mechanically imperfect interface parameters $\alpha=\beta=\gamma=0$ while the dielectrically imperfect interface parameter $\eta \to \infty$ in the mechanically compliant and dielectrically weakly conducting interface discussed in Section 3.1 . This imperfect interface will appear when the actual interphase material between two slabs is nearly insulator. Because the normal components of electric displacements are zero at the interface between slab A slab B, the state vector should be defined as

$$\mathbf{V}(x_i, t) = \{\bar{u}_1, \bar{u}_3, \bar{\sigma}_{33}, \bar{\sigma}_{31}\}^T \tag{29}$$

for in-plane Bloch wave, which lacks $\bar{\varphi}$ and $\bar{D}_3$ compared with the state vector in the perfect interface case. In order to obtain the transfer matrix corresponding to the new state vectors, the boundary conditions $\bar{D}_3 = 0$ at the left and right boundaries of each slab must be used to eliminate the non-independent components U_{17} and U_{18}. Inserting Eq. (11) into $\bar{D}_3 = 0$ leads to

$$\begin{cases} J_7 U_{17} + J_8 U_{18} = -J_1 U_{11} - J_2 U_{12} - J_3 U_{13} - J_4 U_{14} \\ J_7 U_{17} \exp(ik_1\xi_7 d) + J_8 U_{18} \exp(ik_1\xi_8 d) = -J_1 U_{11} \exp(ik_1\xi_1 d) \\ -J_2 U_{12} \exp(ik_1\xi_2 d) - J_3 U_{13} \exp(ik_1\xi_3 d) - J_4 U_{14} \exp(ik_1\xi_4 d) \end{cases} \tag{30}$$

From Eq. (30), the non-independent components U_{17} and U_{18} can be expressed as

$$\begin{cases} U_{17} = M_{11}U_{11} + M_{12}U_{12} + M_{13}U_{13} + M_{14}U_{14} \\ U_{18} = N_{11}U_{11} + N_{12}U_{12} + N_{13}U_{13} + N_{14}U_{14} \end{cases} \tag{31}$$

The grounded metallized interface can be expressed as (Alshits and Shuvalov, 1993)

$$\bar{u}'_i = \bar{u}''_i, \bar{\varphi}' = \bar{\varphi}'' = 0, \bar{\sigma}'_{3i} = \bar{\sigma}''_{3i}, (i = 1, 3) \tag{32}$$

It can also be taken for the limiting case when $\alpha=\beta=\gamma=0$ and $\chi \to \infty$ in the mechanically compliant and dielectrically highly conducting interface. This kind of imperfect interface will appear when the interphase material between two slabs is near conductor grounded. Because the electric potential is zero at interface between slab A slab B, the state vector should also be defined as Eq. (29) for in-plane Bloch wave which lacks $\bar{\varphi}$ and $\bar{D}_3$ compared with the state vector in the perfect interface case. Similarly, in order to obtain the transfer matrix corresponding to the new state vectors, the boundary conditions $\bar{\varphi} = 0$ at the left and right boundaries of slab must be used to eliminate the non-independent components U_{17} and U_{18}. Inserting Eq. (11) into $\bar{\varphi} = 0$ leads to

$$\begin{cases} G_{\varphi 7} U_{17} + G_{\varphi 8} U_{18} = -G_{\varphi 1} U_{11} - G_{\varphi 2} U_{12} - G_{\varphi 3} U_{13} - G_{\varphi 4} U_{14} \\ G_{\varphi 7} U_{17} \exp(ik_1\xi_7 d) + G_{\varphi 8} U_{18} \exp(ik_1\xi_8 d) = -G_{\varphi 1} U_{11} \exp(ik_1\xi_1 d) \\ -G_{\varphi 2} U_{12} \exp(ik_1\xi_2 d) - G_{\varphi 3} U_{13} \exp(ik_1\xi_3 d) - G_{\varphi 4} U_{14} \exp(ik_1\xi_4 d) \end{cases} \tag{33}$$

From Eq. (33), the non-independent components U_{17} and U_{18} can be expressed as

$$\begin{cases} U_{17} = M_{21}U_{11} + M_{22}U_{12} + M_{23}U_{13} + M_{24}U_{14} \\ U_{18} = N_{21}U_{11} + N_{22}U_{12} + N_{23}U_{13} + N_{24}U_{14} \end{cases} \tag{34}$$

By use of Eqs. (31) and (34), the new state vector at the left and at the right boundaries of a slab can be expressed as

$$\mathbf{V}_L(x_3 = 0^+, t) = \mathbf{T}_L\{U_{11}, U_{12}, U_{13}, U_{14}\}^T \exp[\mathbf{i}k_1(x_1 - ct)] \tag{35a}$$

$$\mathbf{V}_R(x_3 = d^-, t) = \mathbf{T}_R\{U_{11}, U_{12}, U_{13}, U_{14}\}^T \exp[\mathbf{i}k_1(x_1 - ct)] \tag{35b}$$

The transfer matrix of a slab is thus obtained by $\mathbf{T} = \mathbf{T}_R\mathbf{T}_L^{-1}$ for the new state vector.

In the case of normal propagation, $\bar{D}_3 = 0$ leads to

$$\Phi_7 = \Phi_8 \tag{36}$$

and $\bar{\varphi} = 0$ leads to

$$\begin{cases} \Phi_7 + \Phi_8 = -(e_{33}/\varepsilon_{33})U_{31} - (e_{33}/\varepsilon_{33})U_{32} \\ (1+d)\Phi_7 + (1-d)\Phi_8 = -(e_{33}/\varepsilon_{33})U_{31}\exp(i\omega d/c_{\mathbf{P}}) \\ \quad -(e_{33}/\varepsilon_{33})U_{32}\exp(-i\omega d/c_{\mathbf{P}}) \end{cases} \tag{37}$$

From Eq. (37), the non-independent components Φ_7 and Φ_8 can be expressed as

$$\begin{cases} \Phi_7 = m_{21}U_{31} + m_{22}U_{32} \\ \Phi_8 = n_{21}U_{31} + n_{22}U_{32} \end{cases} \tag{38}$$

Obviously, the low dielectric interface and grounded metallized interface do not have influence on the dispersion relations of Bloch SV wave and Bloch SH wave. By the use of Eqs. (36) and (38), the new state vectors at the left and at the right boundaries of a slab can be expressed as

$$\mathbf{V}_L(x_3 = 0^+, t) = \mathbf{T}_L\{U_{31}, U_{32}\}^T \exp(-\mathbf{i}\omega t) \tag{39a}$$

$$\mathbf{V}_R(x_3 = d^-, t) = \mathbf{T}_R\{U_{31}, U_{32}\}^T \exp(-\mathbf{i}\omega t) \tag{39b}$$

for Bloch P wave. The transfer matrix for the new state vector can also be obtained by $\mathbf{T} = \mathbf{T}_R\mathbf{T}_L^{-1}$. The explicit expressions of $\mathbf{T}_L$ and $\mathbf{T}_R$ in the low dielectric interface and the grounded metallized interface are given in Appendix C. Recall that the displacement components and the traction components are continuous across the low dielectric interface and the grounded metallized interface. The transfer matrices of these two dielectrically imperfect interfaces are both unit matrices for the new state vector, namely, $\mathbf{T}_\delta = \mathbf{I}$. Therefore, the transfer matrices of a typical single cell can be expressed as

$$\mathbf{T}_{\text{cell}} = \mathbf{T}_\delta\mathbf{T}''\mathbf{T}_\delta\mathbf{T}' = \mathbf{T}''\mathbf{T}' \tag{40}$$

where $\mathbf{T}'$ and $\mathbf{T}''$ are the transfer matrix of slab A and slab B, respectively. Because the state vector is $\mathbf{V}(x_i, t) = \{\bar{u}_1, \bar{u}_3, \bar{\sigma}_{33}, \bar{\sigma}_{31}\}^T$ for in-plane Bloch wave and $\mathbf{V}(x_i, t) = \{\bar{u}_2, \bar{\sigma}_{23}\}^T$ for anti-plane Bloch wave, the transfer matrix of a single cell $\mathbf{T}_{\text{cell}}$ is of 4×4 order for in-plane Bloch wave and 2×2 order for anti-plane Bloch wave. Recall that SH wave is independent of the dielectric parameters of slabs and dielectrically interface conditions, these two dielectrically imperfect interfaces have no effect on the dispersion relations of anti-plane Bloch wave. However, if the isotropic plane ox_1x_2 is selected as the propagation plane, then, the low dielectric interface and grounded metallized interface can influence the dispersion relations of anti-plane Bloch wave.

3.3. Tangent fixed interface and slippery interface conditions

The boundary conditions of the mechanical parallelism of the grounded metallized interface and the low dielectric interface are the tangent fixed interface and the tangent slippery interface. These two mechanically imperfect interfaces can be expressed as

$$\bar{u}_3' = \bar{u}_3'', \bar{u}_i' = \bar{u}_i'' = 0, \bar{\varphi}' = \bar{\varphi}'', \bar{\sigma}_{33}' = \bar{\sigma}_{33}'', \bar{D}_3' = \bar{D}_3'', (i = 1, 2) \tag{41}$$

for the tangent fixed interface and

$$\bar{u}_3' = \bar{u}_3'', \bar{\varphi}' = \bar{\varphi}'', \bar{\sigma}_{33}' = \bar{\sigma}_{33}'', \bar{\sigma}_{3i}' = \bar{\sigma}_{3i}'' = 0, \bar{D}_3' = \bar{D}_3'', (i = 1, 2) \tag{42}$$

for the tangent slippery interface. Because these two imperfect interfaces require $u_2 = 0$ or $\sigma_{23} = 0$, anti-plane Bloch wave can't propagate through these two kinds of interfaces. However, the QP wave and QSV wave can propagate through these interfaces due to the coupled effects between the mechanical fields and the dielectric fields. Because the tangent displacement components or the tangent traction components are zero at the interfaces between slab A and slab B, the state vector should be defined as

$$\mathbf{V}(x_i, t) = \left\{\bar{u}_3, \bar{\varphi}, \bar{\sigma}_{33}, \bar{D}_3\right\}^T \tag{43}$$

for in-plane Bloch wave, which lacks the tangent displacements and tangent traction components compared with the state vector in the perfect interface case. In order to obtain the transfer matrix corresponding to the new state vectors, the boundary conditions $\bar{u}_1 = 0$ or $\bar{\sigma}_{31} = 0$ at the left and at the right boundaries of slab must be used to eliminate the non-independent components U_{17} and U_{18}. Inserting Eq. (11) into $\bar{u}_1 = 0$ or $\bar{\sigma}_{31} = 0$ leads to

$$\begin{cases} U_{17} + U_{18} = -U_{11} - U_{12} - U_{13} - U_{14} \\ U_{17}\exp(ik_1\xi_7 d) + U_{18}\exp(ik_1\xi_8 d) = -U_{11}\exp(ik_1\xi_1 d) \\ \quad -U_{12}\exp(ik_1\xi_2 d) - U_{13}\exp(ik_1\xi_3 d) - U_{14}\exp(ik_1\xi_4 d) \end{cases} \tag{44a}$$

and

$$\begin{cases} H_{17}U_{17} + H_{18}U_{18} = -H_{11}U_{11} - H_{12}U_{12} - H_{13}U_{13} - H_{14}U_{14} \\ H_{17}U_{17}\exp(ik_1\xi_7 d) + H_{18}U_{18}\exp(ik_1\xi_8 d) \\ \quad = -H_{11}U_{11}\exp(ik_1\xi_1 d) \\ \quad -H_{12}U_{12}\exp(ik_1\xi_2 d) - H_{13}U_{13}\exp(ik_1\xi_3 d) \\ \quad -H_{14}U_{14}\exp(ik_1\xi_4 d) \end{cases} \tag{44b}$$

From Eq. (44), the non-independent components U_{17} and U_{18} can be expressed as

$$\begin{cases} U_{17} = M_{31}U_{11} + M_{32}U_{12} + M_{33}U_{13} + M_{34}U_{14} \\ U_{18} = N_{31}U_{11} + N_{32}U_{12} + N_{33}U_{13} + N_{34}U'_{14} \end{cases} \tag{45a}$$

$$\begin{cases} U_{17} = M_{41}U_{11} + M_{42}U_{12} + M_{43}U_{13} + M_{44}U_{14} \\ U_{18} = N_{41}U_{11} + N_{42}U_{12} + N_{43}U_{13} + N_{44}U'_{14} \end{cases} \tag{45b}$$

By the use of Eq. (45), the new state vectors at the left and at the right boundaries of a slab can also be expressed as Eq. (35) The explicit expressions of $\mathbf{T}_L$ and $\mathbf{T}_R$ for the tangent fixed and tangent slippery interface are given in Appendix D.

Because the electric potential, the normal component of electrical displacement and the normal components of mechanical displacement and traction are continuous across interface, the transfer matrices of the tangent fixed and slippery interface are both unit matrix. Therefore, the transfer matrices of a single cell can also be expressed as Eq. (40). In the case of normal propagation, the tangent fixed interface and tangent slippery interface have no influence on the dispersion relations of Bloch P wave but can cut off completely the propagation of Bloch SV wave and Bloch SH wave.

Table 1
Material constants of ALN and CdS.

Mat	Name	C_{11}	C_{12}	C_{13}	C_{33}	C_{44}	ρ	e_{15}	e_{31}	e_{33}	ε_{11}	ε_{33}
A	ALN	410	140	100	390	120	3230	−0.48	−0.58	1.55	7.083	8.411
B	CdS	90.7	58.1	51.0	93.8	15.04	4820	−0.21	−0.24	0.44	798.6	843.7

C_{ij}:GPa, ρ:$kg\,m^{-3}$, e_{ij}: $C\cdot m^{-2}$, ε_{ij}: $10^{-11}C^2\cdot N^{-1}\cdot m^{-2}$.

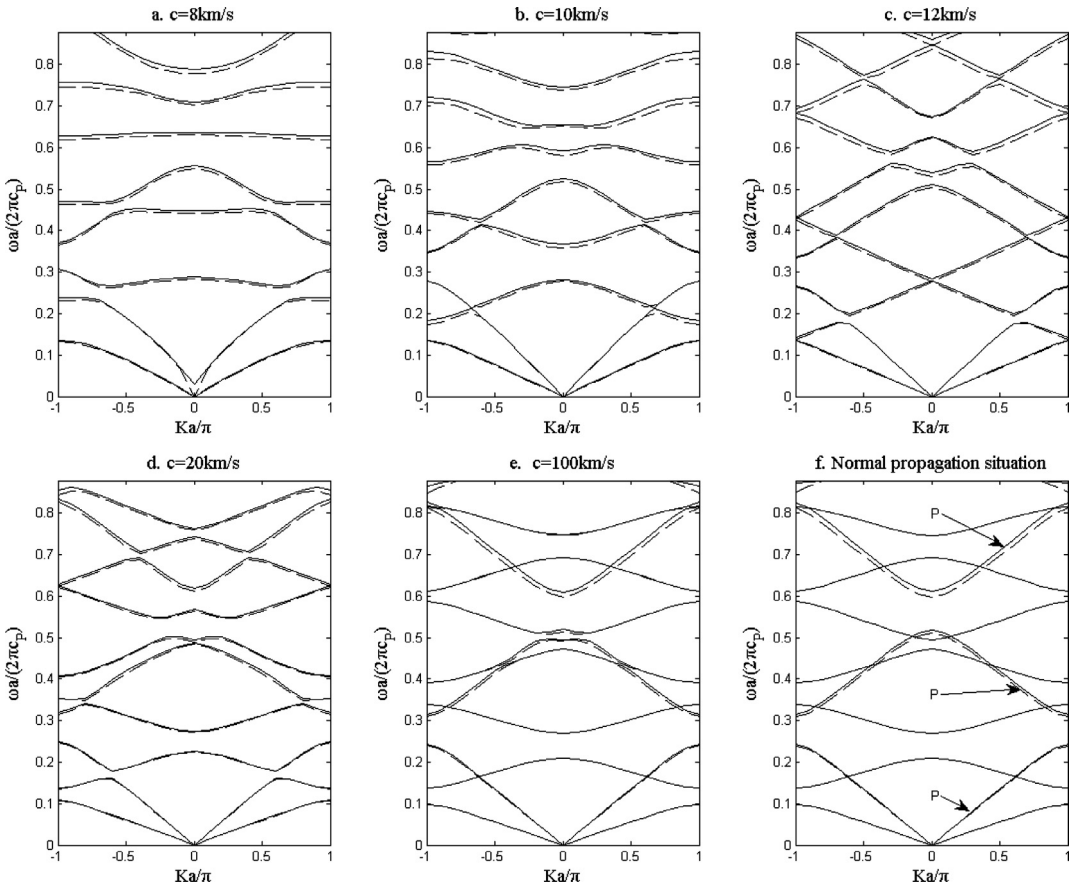

Fig. 2. Effects of the piezoelectricity on dispersion relations of in-plane Bloch waves (with piezoelectric effect, — —without piezoelectric effect).

4. Dispersion equation

After the transfer matrix of coupled waves in a slab and that of the imperfect interfaces between two slabs are both obtained, the state vectors at the left and the right boundaries of a typical single cell in the one-dimensional laminated periodical structure can related by

$$\mathbf{V}'_L\left[x_3=\left(d'+d''\right)^+,t\right]=\mathbf{T}_{cell}\mathbf{V}'_L(x_3=0^+,t)=\mathbf{T}_\delta\mathbf{T}''\mathbf{T}_\delta\mathbf{T}'\mathbf{V}'_L(x_3=0^+,t) \quad (46)$$

On the other hand, according to Bloch theorem on the elastic waves in the periodical structure,

$$\mathbf{V}'_L\left[x_3=\left(d'+d''\right)^+,t\right]=\exp\left[\mathrm{i}K\left(d'+d''\right)\right]\mathbf{V}'_L(x_3=0^+,t) \quad (47)$$

where K is the wavenumber of Bloch wave. Inserting Eq. (46) into Eq. (47) leads to

$$\left\{\mathbf{T}_{\mathbf{cell}}(c,\omega)-\mathbf{I}\exp\left[\mathrm{i}K\left(d'+d''\right)\right]\right\}\mathbf{V}'_L(x_3=0^+,t)=0 \quad (48)$$

where $\mathbf{T}_{\mathbf{cell}}(c,\omega)=\mathbf{T}_\delta\mathbf{T}''\mathbf{T}_\delta\mathbf{T}'$ is the transfer matrix of one typical single cell with the imperfect interfaces which is discussed in Section 3 . The condition of existing non-trivial solution leads to

$$\left|\mathbf{T}_{\mathbf{cell}}(c,\omega)-\mathbf{I}\exp\left[\mathrm{i}K\left(d'+d''\right)\right]\right|=f(c,\omega,K)=0 \quad (49)$$

where $\mathbf{I}$ is a unit matrix. Eq. (49) gives the dispersive relation of Bloch wave in the one-dimensional piezoelectric phononic crystal. The coefficient determinant is a function of c, ω and K. For given c and K, more than one ω can be solved from Eq. (49). Therefore, a group of dispersive curves is obtained in considered frequency range. These dispersive curves divide the frequency range into “passband” and “stopband” alternately.

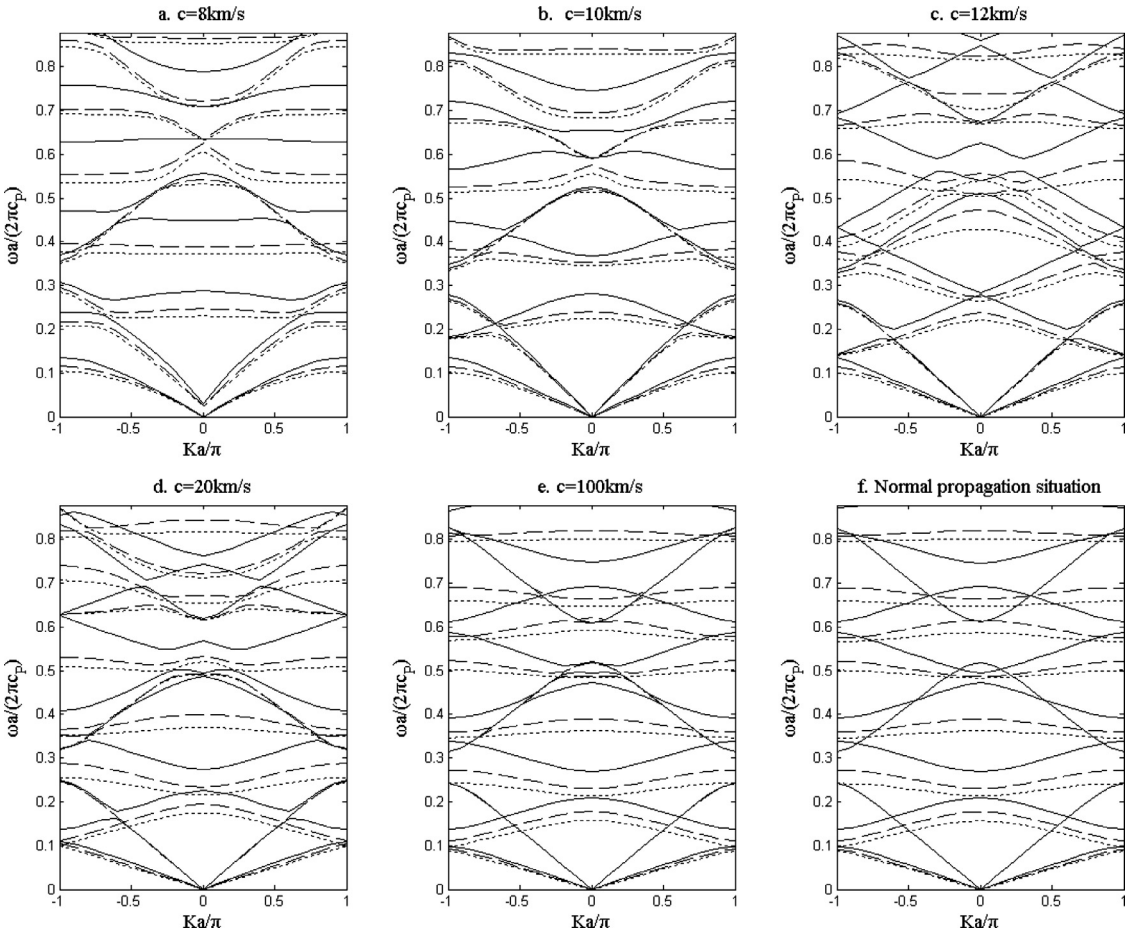

Fig. 3. Effects of the parameter α of the mechanically compliant imperfect interface ($\gamma = 0$, $\eta = 0$ and $\chi = 0$) on dispersion curves of in-plane Bloch waves (——$\alpha = 0$, – –$\alpha = 5 \times 10^{-13}$ $\mathbf{N^{-1}\,m^3}$, ·····$\alpha = 9 \times 10^{-13}$ $\mathbf{N^{-1}\,m^3}$).

For the normal propagation situation, Eq. (49) can be explicitly expressed as

$$\begin{aligned}\cos\left[K\left(d'+d''\right)\right] &= \cos\left(\omega d'/c'_s\right)\cos\left(\omega d''/c''_s\right)\\ &-\tilde{\alpha}\omega\left[\frac{H'}{c'_s}\sin\left(\omega d'/c'_s\right)\cos\left(\omega d''/c''_s\right)\right.\\ &\left.+\frac{H''}{c''_s}\cos\left(\omega d'/c'_s\right)\sin\left(\omega d''/c''_s\right)\right]\\ &-\frac{1}{2}\left(\frac{H'c''_s}{H''c'_s}+\frac{H''c'_s}{H'c''_s}-\tilde{\alpha}^2\frac{H'H''}{c'_s c''_s}\right)\sin\left(\omega d'/c'_s\right)\\ &\sin\left(\omega d''/c''_s\right)\end{aligned} \tag{50}$$

where s =P, $H' = C'_{33} + (e'^2_{33}/\varepsilon'_{33})$, $H'' = C''_{33} + (e''^2_{33}/\varepsilon''_{33})$ and $\tilde{\alpha} = \gamma$ for Bloch P wave; similarly, s =SV, $H' = C'_{44}$, $H'' = C''_{44}$ and $\tilde{\alpha} = \alpha$ for Bloch SV wave; s =SH, $H' = C'_{44}$, $H'' = C''_{44}$ and $\tilde{\alpha} = \beta$ for Bloch SH wave. For the perfect interface, namely, $\tilde{\alpha} = 0$, Eq. (50) can be simplified as

$$\begin{aligned}\cos\left[K\left(d'+d''\right)\right] &= \cos\left(\omega d'/c'_s\right)\cos\left(\omega d''/c''_s\right)\\ &-\frac{1}{2}\left(\frac{H'c''_s}{H''c'_s}+\frac{H''c'_s}{H'c''_s}\right)\sin\left(\omega d'/c'_s\right)\sin\left(\omega d''/c''_s\right)\end{aligned} \tag{51}$$

When one of two piezoelectric slabs is replaced by one isotropic slab and s =SH, Eq. (51) reduces to Eq. (25) in Qian et al (2004b) and Eq. (24) in Lan and Wei (2012). When these two piezoelectric slabs are both replaced by two isotropic slabs, Eq. (51) reduces to Eq. (22) in Zheng and Wei (2009).

5. Numerical results and discussion

In this section, the dispersion curves of in-plane Bloch waves and anti-plane Bloch waves propagating in the one-dimensional piezoelectric phononic crystal are calculated numerically. The material constants of two piezoelectric solids in phononic crystal, aluminum nitride (ALN) (Abd-alla and Alsheikh, 2009) and cadmium sulfide (CdS) (Auld, 1990) are listed in Table 1. The length ratio of two piezoelectric solids in a single cell are $d'/d'' = 1$ and total length of single cell is $a = d' + d''$. In order to investigate the influences of imperfect interfaces, dispersion curves for the imperfect interfaces and the perfect interface are both calculated and shown in same figure to facilitate the comparison. The dispersion curves are drawn in first Brilouin zone, namely, the dimensionless Bloch wavenumber $Ka/\pi \in [-1, 1]$.

5.1. In-plane Bloch wave

The piezoelectric effects on dispersion curves of in-plane Bloch waves are shown in Fig. 2. Fig. 2(a)–(e)

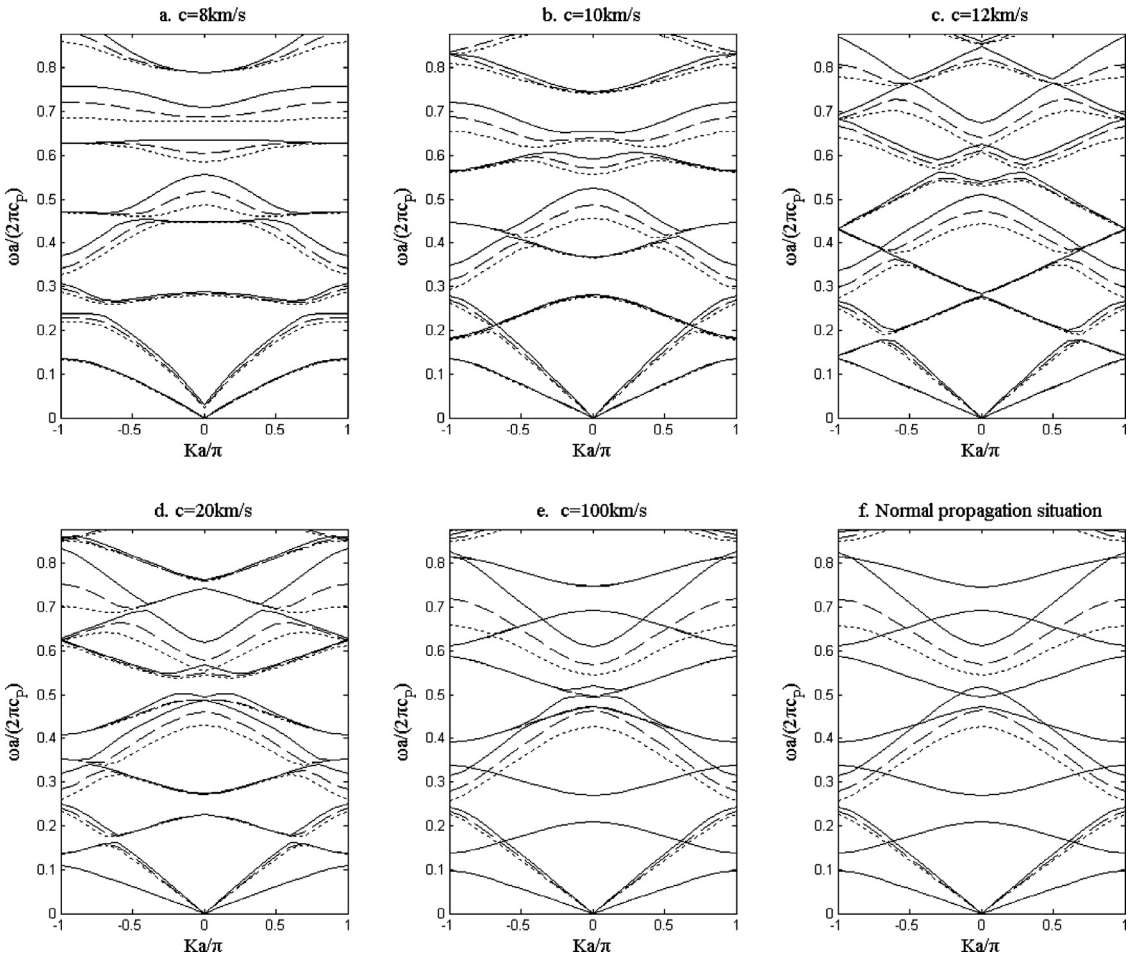

Fig. 4. Effects of the parameter γ of the mechanically compliant imperfect interface ($\alpha = 0$, $\eta = 0$ and $\chi = 0$) on dispersion curves of in-plane Bloch waves ($--\gamma = 0, - -\gamma = 5 \times 10^{-14}\,\mathbf{N^{-1}\,m^3}$, $\cdots\cdots\gamma = 9 \times 10^{-14}\,\mathbf{N^{-1}\,m^3}$).

shows the dispersive curves of in-plane Bloch waves in the oblique propagation situation. Fig. 2(f) shows the dispersive curves of in-plane Bloch waves in the normal propagation situation. Physically, in-plane Bloch waves in the oblique propagation situation are formed by interfering of QP wave and QSV wave which are coupled together. When c increases, namely, the propagation direction of QP wave and QSV trends to the normal of interface gradually, the coupled QP wave and QSV wave decouple or split gradually. In the limiting case corresponding with $c \to \infty$, that is the normal propagation situation, QP wave and QSV wave split completely and reduce to the P wave and SV wave. Fig. 2(f) shows the dispersive curves of Bloch P wave and Bloch SV wave which are decoupled in the normal propagation situation. Bloch P wave are formed only by the interfering P waves while Bloch SV wave are formed only by interfering SV waves. Fig. 2(a)–e) shows the evolutionary decoupling process of QP wave with QSV wave. The fact that this evolutionary process tends to the normal propagation situation gradually as $c \to \infty$ validate our numerical results in the oblique propagation situation. In the oblique propagation situation, the piezoelectric effect has influences on both QP and QSV waves while has only influences on P wave in the normal propagation situation. No matter normal or oblique propagation situation, the piezoelectric effect has more evident influences on high frequency Bloch waves than on low frequency Bloch waves.

The Influences of the parameter α and γ of the mechanically compliant imperfect interface on dispersion curves of in-plane Bloch waves are shown in Figs. 3 and 4. It is observed that the increase of the mechanical parameter α and γ makes the dispersion curves shifting toward low frequency. This phenomenon is due to the fact that the flexibility increases for the periodic structure with imperfect interfaces compared with that with perfect interfaces. Because the mechanical parameter α only affects the tangent flexibility while the mechanical parameter γ only affects the normal flexibility of periodic structure, it is observed that the mechanical parameter α only affects Bloch SV wave while the mechanical parameter γ only affects the Bloch P wave in the normal propagation situation, see Figs. 3(f) and 4(f). However, in the oblique propagation situation, both mechanical parameter α and γ have influences on dispersive curves of Bloch waves, but the influences of the mechanical parameter α and

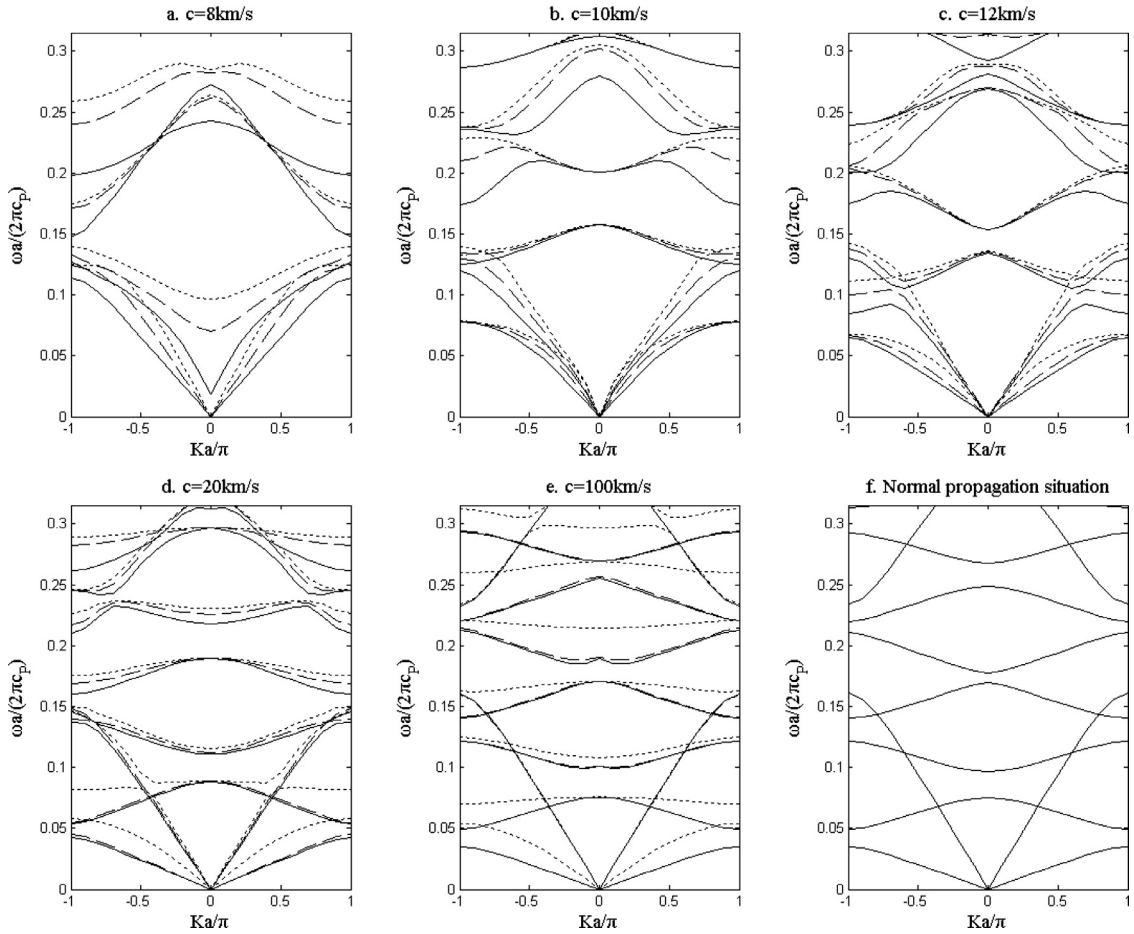

Fig. 5. Effects of the parameter η (——$\eta = 0$, – –$\eta = 1 \times 10^7 \mathbf{Nm^3C^{-2}}$) of the weakly conducting imperfect interface ($\alpha = 0, \gamma = 0$) and the low dielectric interface (·····Low) on dispersion curves of in-plane Bloch wave.

γ are different at different range of Brilouin zone. This can be explained by that the Bloch waves in oblique propagation situation are created by QP waves with QSV waves which are coupled together. The mechanical parameter α has more evident influence than the mechanical parameter γ at the range where the QSV wave dominates in Bloch wave while the mechanical parameter γ has more evident influence than the mechanical parameter α at the range where the QP wave dominates in Bloch wave. However, no matter parameter α and γ, the influences of these mechanical parameter become more evident on the high frequency dispersive curves compared with the low frequency dispersive curves.

The influences of dielectric parameter η and χ in the weakly conducting and high highly conducting imperfect interfaces on the dispersive curves of in-plane Bloch waves are much smaller than that of the mechanical parameter α and γ such that the deviations are nearly unnoticed. This is because the mechanical energy dominates and the electric energy is secondary in the total energy carried by the Bloch waves in piezoelectric slab. In order to enhance the influence of dielectrically imperfect interfaces, the piezoelectric and dielectric parameters of slab A and slab B are factitiously increased by 100 times in the present numerical calculation. The effects of the parameter η and χ are shown in Figs. 5 and 6, respectively. It is observed that the increasing of the parameter η makes the dispersive curves of in-plane Bloch waves shifting toward high frequency. In contrast, the increasing of the parameter χ makes the dispersive curves of in-plane Bloch waves shifting toward low frequency. It is also observed that, different from the parameter α and γ in the mechanically imperfect interface, the influences of the parameter η and χ decrease gradually as c increase. In the limiting case, i.e. the normal propagation situation, the parameter η and χ do not have any influence on the dispersive curves of in-plane Bloch waves. The low dielectric interface and the grounded metallized interface have completely opposite influences on the dispersive curves in the oblique propagation situation. The dispersive curves shift toward high frequency for the low dielectric interface but shift toward low frequency for the grounded metallized interface. This observation can be explained by that the low dielectric interface can be taken as the limiting case of the dielectrically weakly conducting interface while the grounded metallized interface the limiting case of the dielectrically highly conducting interface. In the normal propagation situation, the low dielectric interface

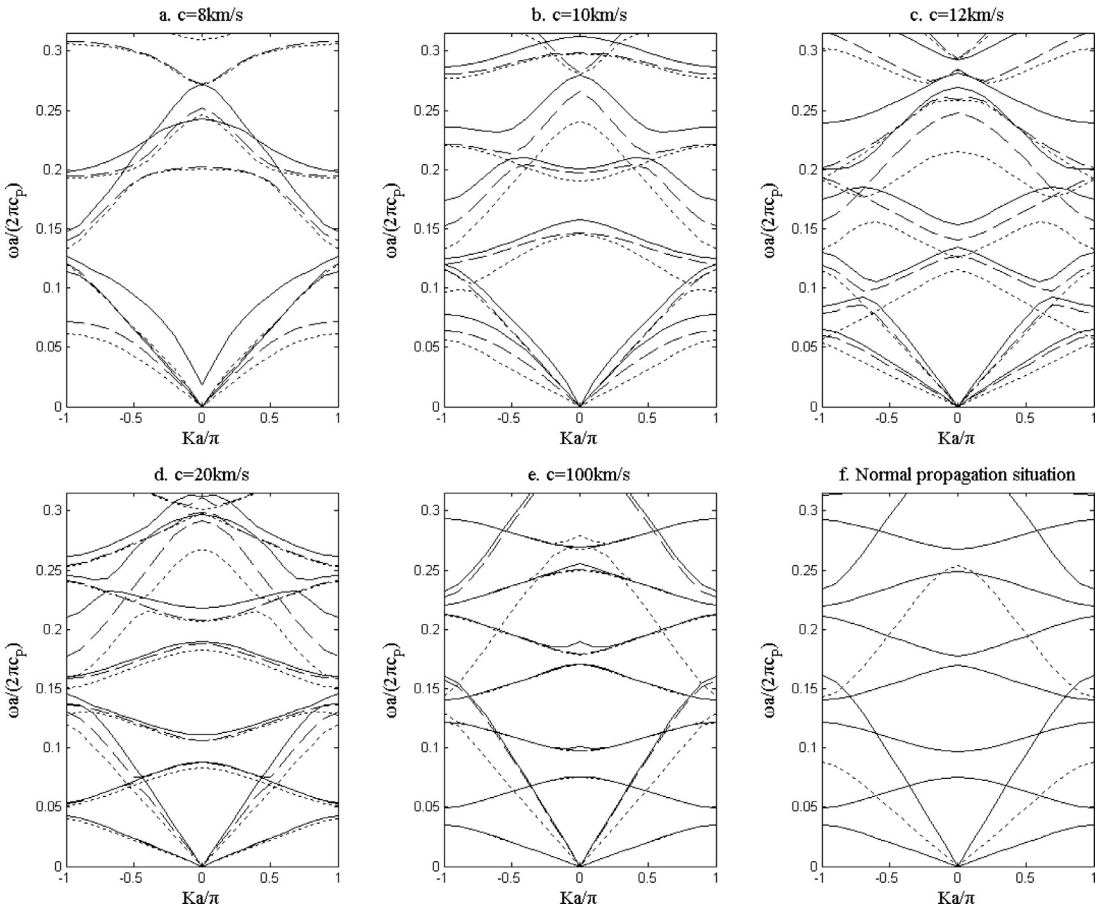

Fig. 6. Effects of the parameter χ (——$\chi = 0$, – – $\chi = 5 \times 10^{-9}\mathbf{N^{-1}m^{-1}C^2}$) of the highly conducting imperfect interface ($\alpha = 0$, $\gamma = 0$) and the grounded metallized interface (·····Gro) on dispersive curves of in-plane Bloch wave.

does not have any influence on the dispersive curves of Bloch P wave and Bloch SV wave. However, the grounded metallized interfaces still have evident influences on the dispersive curves of the Bloch P waves. The band gap is defined as the gap between two adjacent dispersive curves in Brilouin zone. Since the dispersive curves are affected by the dielectric imperfect interfaces, the band gaps are therefore dependent of the dielectric imperfect interface. It is observed that the band gap between two adjacent dispersive curves of Bloch P waves in the normal propagation situation shift drastically toward to low frequency for grounded metallized interfaces compared with the perfect interface. This phenomenon may be used to design the vibration isolator at low frequency.

As the mechanical parallelism of the low dielectric interface and the grounded metallized interface, the influences of the tangent fixed interface and the tangent slippery interface on dispersion curves of in-plane Bloch waves are also calculated and are shown in Fig. 7. In the oblique propagation situation, in-plane Bloch wave includes QP wave component and QSV wave component. The QP wave component is same for the tangent fixed interface and tangent slippery interface; but the QSV component is different for the tangent fixed interface and the tangent slippery interface. This results in the differences of dispersive curves corresponding with tangent fixed interface and tangent slippery interface. When c increases, the propagation directions of both QP wave and QSV wave tend to normal of interface gradually. The differences of dispersive curves corresponding with the tangent fixed interface and tangent slippery interface disappear gradually. In the limiting case of $c \to \infty$, namely, the normal propagation situation, the tangent fixed interface and the tangent slippery interface have completely same dispersive curves. Furthermore, only the dispersive curves corresponding P waves are retained in the normal propagation situation because the SV wave cannot propagate through either the tangent fixed interface or the tangent slippery interface. It is also observed that QP wave decouples with QSV wave gradually with the increase of c. And the dispersive curves corresponding with QSV waves become flat line in total Brillouin zone for the tangent fixed interface and the tangent slippery interface. This is because SV wave cannot propagate through these two kinds of interfaces in the limiting case of $c \to \infty$. And QSV wave gradually becomes into the standing wave from the propagating wave. In normal propagation situation, QP waves become into P waves while QSV waves disappears completely. As a result, the differences of dispersive curves corresponding with the tangent fixed interface and tangent slippery interface disappear completely.

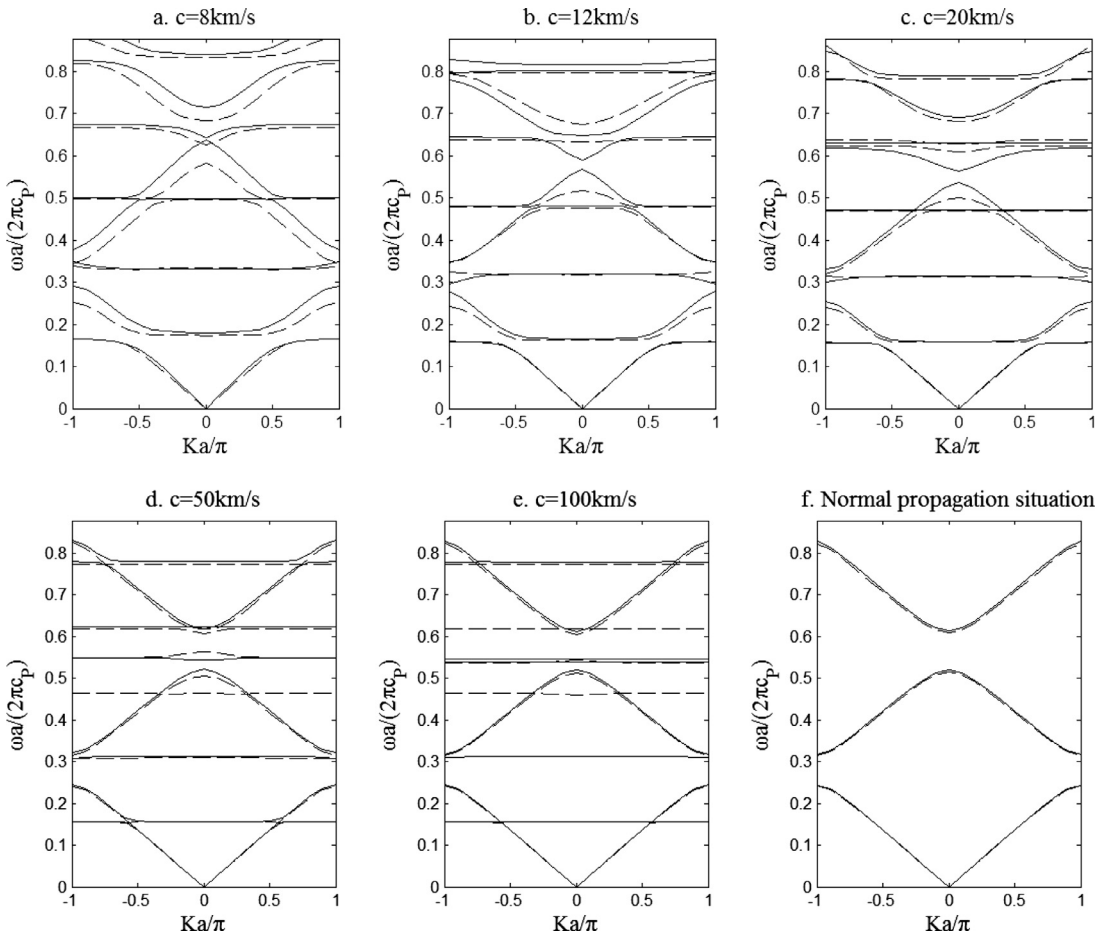

Fig. 7. Effects of the tangent fixed interface and the tangent slippery interface on dispersion curves of in-plane Bloch waves (——Fixed, — —Slip).

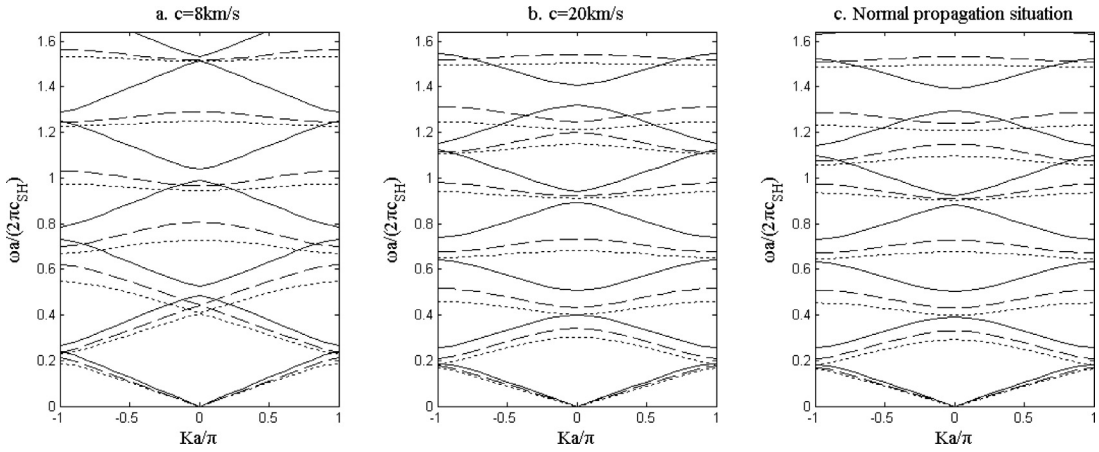

Fig. 8. Effects of the parameter β of the compliant imperfect interface on dispersion curves of anti-plane Bloch waves (——$\beta = 0$, — —$\beta = 5 \times 10^{-13}\mathbf{N^{-1}m^3}$, ·····$\beta = 9 \times 10^{-13}\mathbf{N^{-1}m^3}$).

5.2. Anti-plane Bloch wave

The dielectric imperfect interfaces do not have any influence on the SH wave. The tangent fixed interface and the tangent slippery interface can cut off the propagation of SH waves completely, no matter the oblique or normal propagation situation. Therefore, only mechanical compliant imperfect interface needs to be considered. The influences of the parameter β of the mechanically compliant imperfect interface on dispersion curves of anti-plane Bloch wave are

calculated and are shown in Fig. 8. It is observed that the dispersion curves shift toward low frequency as the increase of the parameter β no matter the oblique propagation and normal propagation. This is due to the fact the mechanical compliant imperfect interface increases the flexibility of the periodical structures. It is also observed that the influences of parameter β are more evident on the high frequency dispersive curves than on the low frequency dispersive curves. The influences of parameter β on the anti-plane Bloch waves are similar with the influences of parameter α and γ on the in-plane Bloch waves.

6. Conclusions

The influences of mechanical and dielectrical imperfect interface on the dispersion relations of Bloch waves in one-dimensional piezoelectric phononic crystal are the main concerns of the present work. The oblique propagation situation and the normal propagation situations are both considered. Four kinds of mechanical imperfect interfaces, namely, the normal compliant interface, the tangent compliant interface, the tangent fixed interface and tangent slippery interface, and four kinds of dielectric imperfect interfaces, namely, the weak conducting interface, the high conducting interface, the low dielectric interface and the grounded metallized interface, are investigated. The dispersive curves of in-plane and anti-plane Bloch waves are calculated and shown in the Brillouin zone. From the numerical results, the following conclusions can be drawn:

(1) In oblique propagation situation, the piezoelectric effect has influences on both QP and QSV waves while has only influences on P wave in normal propagation situation. No matter normal or oblique propagation situation, the piezoelectric effect has more evident influences on high frequency Bloch waves than on low frequency Bloch waves.
(2) In-plane Bloch waves in the oblique propagation situation are formed by interfering of QP waves and QSV waves which are coupled together. When c increases, the coupled QP waves and QSV waves decouple gradually and decouple completely in the normal propagation situation. In-plane Bloch waves in the oblique propagation situation reduce to the Bloch P waves and Bloch SV waves in the normal propagation. The Bloch SH waves do not couple with in-plane Bloch waves in both the oblique propagation situation and the normal propagation situation.
(3) The mechanical imperfect interfaces have more evident influences on the dispersive curves of Bloch waves than the dielectric imperfect interfaces. No matter the mechanical imperfect interfaces and the dielectric imperfect interfaces, their influences are more evident on the high frequency dispersive curves than on the low frequency dispersive curves.
(4) Both the mechanical tangent imperfect interface and the mechanical normal imperfect interface have influences on in-plane Bloch waves in the oblique propagation situation and these mechanical compliant interfaces make the dispersion curves shifting toward low frequency. The mechanical tangent imperfect interface only affects Bloch SV waves while the mechanical normal imperfect interface only affects the Bloch P waves in the normal propagation situation.
(5) The weakly conducting interface makes the dispersive curves of Bloch waves shifting toward high frequency while the highly conducting interface makes the dispersive curves shifting toward low frequency. But their influences decrease gradually as c increases. In the normal propagation situation, the weakly conducting and highly conducting interfaces do not have any influence on the dispersive curves.
(6) The low dielectric interface and the grounded metallized interface have completely opposite influences on the dispersive curves in the oblique propagation situation. The dispersive curves shift toward high frequency for the low dielectric interface but shift toward low frequency for the grounded metallized interface. In the normal propagation situation, the low dielectric interface does not have influences on Bloch waves while the grounded metallized interfaces affects only Bloch P waves and makes the dispersive curves shifting toward to low frequency drastically.
(7) The dispersive curves corresponding with the tangent fixed interface and tangent slippery interface are different in the oblique propagation situation but are same in the normal propagation situation. Only the dispersive curves corresponding P waves are retained in the normal propagation situation. The dispersive curves corresponding with QSV waves become gradually the flat line in total Brillouin zone for the tangent fixed interface and the tangent slippery interface as c increases. This means the QSV wave becomes gradually into standing waves.
(8) The mechanical compliant imperfect interface makes the dispersive curves of the Bloch SH wave shifting toward low frequency. The dielectric imperfect interfaces do not have any influence on the dispersive curves of the Bloch SH wave. The tangent fixed interface and the tangent slippery interface can cut off the propagation of Bloch SH waves completely, no matter the oblique or normal propagation.

Acknowledgments

The work is supported by the National Natural Science Foundation of China (No. 10972029) and Opening fund of State Key Laboratory of Nonlinear Mechanics (LNM).

Appendix A

The explicit expressions of W_{ij} in Eq. (5) are

$$W_{11} = C_{11} + C_{44}\xi^2 - \rho c^2,\ W_{22} = C_{66} + C_{44}\xi^2 - \rho c^2,$$
$$W_{33} = C_{44} + C_{33}\xi^2 - \rho c^2, W_{44} = -\left(\varepsilon_{11} + \varepsilon_{33}\xi^2\right),$$
$$W_{13} = W_{31} = (C_{44} + C_{13})\xi,\ W_{14} = W_{41} = (e_{31} + e_{15})\xi,$$
$$W_{34} = W_{43} = e_{15} + e_{33}\xi^2,$$
$$W_{12} = W_{21} = W_{23} = W_{32} = W_{24} = W_{42} = 0.$$

The explicit expressions of $\hat{W}_{ij}$ in Eq. (7) are

$$\hat{W}_{11} = C_{11} + C_{66}\xi^2 - \rho c^2,\ \hat{W}_{22} = C_{66} + C_{11}\xi^2 - \rho c^2,$$
$$\hat{W}_{33} = C_{44} + C_{44}\xi^2 - \rho c^2, \hat{W}_{44} = -\left(\varepsilon_{11} + \varepsilon_{11}\xi^2\right),$$

$$\hat{W}_{12} = \hat{W}_{21} = (C_{12} + C_{66})\xi,\ \hat{W}_{34} = \hat{W}_{43} = e_{15} + e_{15}\xi^2,$$
$$\hat{W}_{13} = \hat{W}_{14} = \hat{W}_{23} = \hat{W}_{24} = \hat{W}_{31} = \hat{W}_{32} = \hat{W}_{41} = \hat{W}_{42} = 0.$$

Appendix B

In the oblique propagation situation, the matrix $\mathbf{T}_L$ and $\mathbf{T}_R$ are

$$T_{L1p} = 1,\ T_{L2p} = G_{3q},\ T_{L3p} = G_{\varphi q},\ T_{L4p} = ik_1H_{3q},$$
$$T_{L5p} = ik_1H_{1q},\ T_{L6p} = ik_1J_q,\ T_{R1p} = \exp(ik_1\xi_q d),$$
$$T_{R2p} = G_{3q}\exp(ik_1\xi_q d),\ T_{R3p} = G_{\varphi q}\exp(ik_1\xi_q d),$$
$$T_{R4p} = ik_1H_{3q}\exp(ik_1\xi_q d),\ T_{R5p} = ik_1H_{1q}\exp(ik_1\xi_q d),$$
$$T_{R6p} = ik_1J_q\exp(ik_1\xi_q d),$$

where $p = q$ when $p = 1, 2, 3, 4$, $q = 7$ when $p = 5$ and $q = 8$ when $p = 6$ for in-plane Bloch wave,

$$\mathbf{T}_L = \begin{bmatrix} 1 & 1 \\ ik_1C_{44}\xi_5 & ik_1C_{44}\xi_6 \end{bmatrix},$$
$$\mathbf{T}_R = \begin{bmatrix} \exp(ik_1\xi_5 d) & \exp(ik_1\xi_6 d) \\ ik_1C_{44}\xi_5\exp(ik_1\xi_5 d) & ik_1C_{44}\xi_6\exp(ik_1\xi_6 d) \end{bmatrix},$$

for anti-plane Bloch wave. In the normal propagation situation,

$$T_{L11} = T_{L12} = 1,\ T_{L13} = T_{L14} = 0,\ T_{L21} = T_{L22} = e_{33}/\varepsilon_{33},$$
$$T_{L23} = T_{L24} = 1, T_{L31} = -T_{L32} = i(\omega/c_P)\left[C_{33} + \left(e_{33}^2/\varepsilon_{33}\right)\right],$$
$$T_{L33} = -T_{L34} = e_{33},\ T_{L41} = T_{L42} = 0, T_{L43} = -T_{L44} = -\varepsilon_{33},$$
$$T_{R11} = \exp(i\omega d/c_P),\ T_{R12} = \exp(-i\omega d/c_P),\ T_{R13} = T_{R14} = 0,$$
$$T_{R21} = (e_{33}/\varepsilon_{33})\exp(i\omega d/c_P), T_{R22} = (e_{33}/\varepsilon_{33})\exp(-i\omega d/c_P),$$
$$T_{R23} = 1 + d, T_{R24} = 1 - d,\ T_{R31} = i(\omega/c_P)\left[C_{33} + \left(e_{33}^2/\varepsilon_{33}\right)\right]\exp(i\omega d/c_P), T_{R32} = -i(\omega/c_P)\left[C_{33} + \left(e_{33}^2/\varepsilon_{33}\right)\right]\exp(-i\omega d/c_P),\ T_{R33} = -T_{R34} = e_{33},\ T_{R41} = T_{R42} = 0,$$
$$T_{R43} = -T_{R44} = -\varepsilon_{33},$$

for Bloch P wave,

$$\mathbf{T}_L = \begin{bmatrix} 1 & 1 \\ i(\omega/c_{SV})C_{44} & -i(\omega/c_{SV})C_{44} \end{bmatrix},$$
$$\mathbf{T}_R = \begin{bmatrix} \exp(i\omega d/c_{SV}) & \exp(-i\omega d/c_{SV}) \\ i(\omega/c_{SV})C_{44}\exp(i\omega d/c_{SV}) & -i(\omega/c_{SV})C_{44}\exp(-i\omega d/c_{SV}) \end{bmatrix},$$

for Bloch SV wave and

$$\mathbf{T}_L = \begin{bmatrix} 1 & 1 \\ i(\omega/c_{SH})C_{44} & -i(\omega/c_{SH})C_{44} \end{bmatrix},$$
$$\mathbf{T}_R = \begin{bmatrix} \exp(i\omega d/c_{SH}) & \exp(-i\omega d/c_{SH}) \\ i(\omega/c_{SH})C_{44}\exp(i\omega d/c_{SH}) & -i(\omega/c_{SH})C_{44}\exp(-i\omega d/c_{SH}) \end{bmatrix},$$

for Bloch SH wave.

Appendix C

In cases of low dielectric interface and grounded metallized interface, the elements of matrix $\mathbf{T}_L$ and $\mathbf{T}_R$ are

$$T_{L1q} = 1 + M_{pq} + N_{pq},\ T_{L2q} = G_{3q} + G_{37}M_{pq} + G_{38}N_{pq},$$
$$T_{L3q} = ik_1(H_{3q} + H_{37}M_{pq} + H_{38}N_{pq}),$$
$$T_{L4q} = ik_1(H_{1q} + H_{17}M_{pq} + H_{18}N_{pq}),$$
$$T_{R1q} = \exp(ik_1\xi_q d) + \exp(ik_1\xi_7 d)M_{pq} + \exp(ik_1\xi_8 d)N_{pq},$$
$$T_{R2q} = G_{3q}\exp(ik_1\xi_q d) + G_{37}\exp(ik_1\xi_7 d)M_{pq} + G_{38}\exp(ik_1\xi_8 d)N_{pq},\ T_{R3q} = ik_1\left[H_{3q}\exp(ik_1\xi_q d) + H_{37}\exp(ik_1\xi_7 d)M_{pq} + H_{38}\exp(ik_1\xi_8 d)N_{pq}\right],$$
$$T_{R4q} = ik_1\left[H_{1q}\exp(ik_1\xi_q d) + H_{17}\exp(ik_1\xi_7 d)M_{pq} + H_{18}\exp(ik_1\xi_8 d)N_{pq}\right],$$

where $q = 1, 2, 3, 4$, $p = 1$ when the interface is the low dielectric interface and $p = 2$ when the interface is the grounded metallized interface. In the case of normal propagation,

$$T_{L11} = T_{L12} = 1,\ T_{L21} = -T_{L22} = i(\omega/c_P)\left[C_{33} + \left(e_{33}^2/\varepsilon_{33}\right)\right],$$
$$T_{R11} = \exp(i\omega d/c_P), T_{R12} = \exp(-i\omega d/c_P),$$
$$T_{R21} = i(\omega/c_P)\left[C_{33} + \left(e_{33}^2/\varepsilon_{33}\right)\right]\exp(i\omega d/c_P),$$
$$T_{R22} = -i(\omega/c_P)\left[C_{33} + \left(e_{33}^2/\varepsilon_{33}\right)\right]\exp(-i\omega a/c_P),$$

for the low dielectric interface and

$$T_{L11} = T_{L12} = 1,\ T_{L21} = i(\omega/c_P)\left[C_{33} + \left(e_{33}^2/\varepsilon_{33}\right)\right] + e_{33}(m_{21} - n_{21}), T_{L22} = -i(\omega/c_P)\left[C_{33} + \left(e_{33}^2/\varepsilon_{33}\right)\right] + e_{33}(m_{22} - n_{22}),\ T_{R11} = \exp(i\omega d/c_P),$$
$$T_{R12} = \exp(-i\omega d/c_P),\ T_{R21} = i(\omega/c_P)\left[C_{33} + \left(e_{33}^2/\varepsilon_{33}\right)\right]\exp(i\omega d/c_P) + e_{33}(m_{21} - n_{21}),$$
$$T_{R22} = -i(\omega/c_P)\left[C_{33} + \left(e_{33}^2/\varepsilon_{33}\right)\right]\exp(-i\omega d/c_P) + e_{33}(m_{22} - n_{22}),$$

for the grounded metallized interface. The explicit expressions of M_{pq} and N_{pq} are

$$\begin{bmatrix} M_{11} & M_{12} & M_{13} & M_{14} \\ N_{11} & N_{12} & N_{13} & N_{14} \end{bmatrix} = -\begin{bmatrix} J_7 & J_8 \\ J_7\exp(\mathbf{i}k_1\xi_7 d) & J_8\exp(\mathbf{i}k_1\xi_8 d) \end{bmatrix}^{-1} \cdot \begin{bmatrix} J_1 & J_2 & J_3 & J_4 \\ J_1\exp(\mathbf{i}k_1\xi_1 d) & J_2\exp(\mathbf{i}k_1\xi_2 d) & J_3\exp(\mathbf{i}k_1\xi_3 d) & J_4\exp(\mathbf{i}k_1\xi_4 d) \end{bmatrix},$$
$$\begin{bmatrix} M_{21} & M_{22} & M_{23} & M_{24} \\ N_{21} & N_{22} & N_{23} & N_{24} \end{bmatrix} = -\begin{bmatrix} G_{\varphi 7} & G_{\varphi 8} \\ G_{\varphi 7}\exp(\mathbf{i}k_1\xi_7 d) & G_{\varphi 8}\exp(\mathbf{i}k_1\xi_8 d) \end{bmatrix}^{-1} \cdot \begin{bmatrix} G_{\varphi 1} & G_{\varphi 2} & G_{\varphi 3} & G_{\varphi 4} \\ G_{\varphi 1}\exp(\mathbf{i}k_1\xi_1 d) & G_{\varphi 2}\exp(\mathbf{i}k_1\xi_2 d) & G_{\varphi 3}\exp(\mathbf{i}k_1\xi_3 d) & G_{\varphi 4}\exp(\mathbf{i}k_1\xi_4 d) \end{bmatrix}.$$

The explicit expressions of m_{2q} and n_{2q} are

$$\begin{bmatrix} m_{21} & m_{22} \\ n_{21} & n_{22} \end{bmatrix} = -(e_{33}/\varepsilon_{33})\begin{bmatrix} 1 & 1 \\ 1 + d & 1 - d \end{bmatrix}^{-1} \cdot \begin{bmatrix} 1 & 1 \\ \exp(i\omega d/c_P) & \exp(-i\omega d/c_P) \end{bmatrix}.$$

Appendix D

In cases of tangent fixed interface and slippery interface, the elements of matrix $\mathbf{T}_L$ and $\mathbf{T}_R$ are

$$T_{L1q} = G_{3q} + G_{37}M_{pq} + G_{38}N_{pq},\ T_{L2q} = G_{3q} + G_{37}M_{pq} + G_{38}N_{pq}, T_{L3q} = ik_1(H_{3q} + H_{37}M_{pq} + H_{38}N_{pq}),$$
$$T_{L4q} = ik_1(J_q + J_7M_{pq} + J_8N_{pq}), T_{R1q} = G_{3q}\exp(ik_1\xi_q d)$$

$$+G_{37}\exp(ik_1\xi_7 d)M_{pq}+G_{38}\exp(ik_1\xi_8 d)N_{pq},$$

$$T_{R2q}=G_{\varphi j}\exp(ik_1\xi_q d)+G_{\varphi 7}\exp(ik_1\xi_7 d)M_{pq}$$
$$+G_{\varphi 8}\exp(ik_1\xi_8 d)N_{pq},\ T_{R3q}=ik_1\left[H_{3q}\exp(ik_1\xi_q d)\right.$$
$$\left.+H_{37}\exp(ik_1\xi_7 d)M_{pq}+H_{38}\exp(ik_1\xi_8 d)N_{pq}\right],$$

$$T_{R4q}=ik_1[J_q\exp(ik_1\xi_q d)+J_7\exp(ik_1\xi_7 d)M_{pq}$$
$$+J_8\exp(ik_1\xi_8 d)N_{pq}],$$

where $q=1,2,3,4$, $p=3$ when the interface is the tangent fixed interface while $p=4$ when the interface is the tangent slippery interface. The explicit expressions of M_{pq} and N_{pq} are

$$\begin{bmatrix}M_{31} & M_{32} & M_{33} & M_{34}\\ N_{31} & N_{32} & N_{33} & N_{34}\end{bmatrix}=-\begin{bmatrix}1 & 1\\ \exp(\mathbf{i}k_1\xi_7 d) & \exp(\mathbf{i}k_1\xi_8 d)\end{bmatrix}^{-1}$$
$$\cdot\begin{bmatrix}1 & 1 & 1 & 1\\ \exp(\mathbf{i}k_1\xi_1 d) & \exp(\mathbf{i}k_1\xi_2 d) & \exp(\mathbf{i}k_1\xi_3 d) & \exp(\mathbf{i}k_1\xi_4 d)\end{bmatrix},$$

$$\begin{bmatrix}M_{41} & M_{42} & M_{43} & M_{44}\\ N_{41} & N_{42} & N_{43} & N_{44}\end{bmatrix}=-\begin{bmatrix}H_{17} & H_{18}\\ H_{17}\exp(\mathbf{i}k_1\xi_7 d) & H_{18}\exp(\mathbf{i}k_1\xi_8 d)\end{bmatrix}^{-1}$$
$$\cdot\begin{bmatrix}H_{11} & H_{12} & H_{13} & H_{14}\\ H_{11}\exp(\mathbf{i}k_1\xi_1 d) & H_{12}\exp(\mathbf{i}k_1\xi_2 d) & H_{13}\exp(\mathbf{i}k_1\xi_3 d) & H_{14}\exp(\mathbf{i}k_1\xi_4 d)\end{bmatrix}.$$

References

Abd-alla, A.N., Alsheikh, F.A., 2009. Reflection and refraction of plane quasi-longitudinal waves at an interface of two piezoelectric media under initial stresses. Arch. Appl. Mech. 79, 843–857.

Alshits, V.I., Shuvalov, A.L., 1993. Bragg reflection of sound in a periodic structure of piezoelectric-crystal layers with superconducting or metalized interlayers. J. Exp. Theor. Phys. 103, 1356–1370.

Alshits, V.I., Shuvalov, A.L., 1995. Resonance reflection and transmission of shear elastic waves in multilayered piezoelectric structures. J. Appl. Phys. 77, 2659–2665.

Alvarez-Mesquida, A.A., Rodriguez-Ramos, R., Comas, F., Monsivais, G., Esquivel-Sirvent, R., 2001. Scattering of shear horizontal piezoelectric waves in piezocomposite media. J. Appl. Phys. 89 (5), 2886–2892.

Auld, B.A., 1990. Acoustic Fields and Waves in Solids. Kriger PublishingCompany, Malabar.

Chen, A.-Li, Wang, Yue-Sheng, 2007. Study on band gaps of elastic waves propagating in one-dimensional disordered phononic crystals. Physica B 392, 369–378.

Fan, Hui, Yang, Jiashi, Xu, Limei, 2006. Piezoelectric waves near an imperfectly bonded interface between two half-spaces. Appl. Phys. Lett 88, 203509.

Huang, Y., Li, X.F., Lee, K.Y., 2009. Interfacial shear horizontal (SH) wave propagating in a two-phase piezoelectric/piezomagnetic structure with an imperfect interface. Philos. Mag. Lett. 89, 95–103.

Kafesaki, M., Sigalas, M.M., Economou, E.N., 1995. Elastic wave band gaps in 3-D periodic polymer matrix. Solid State Commun. 96 (5), 285–289.

Kushwaha, M.S., Halevi, P., Dobrzynski, L., et al., 1993. Acoustic band structure of periodic elastic composites. Phys. Rev. Lett. 71 (13), 2022–2025.

Lan, Man, Wei, Peijun, 2012. Laminated piezoelectric phononic crystal with imperfect interfaces. J. Appl. Phys. 111 013505~1-9.

Lan, Man, Wei, Peijun, 2014. Band gap of piezoelectric/piezomagnetic phononic crystal with graded interlayer. Acta Mech. 225, 1779–1794.

Liu, Z.Y., Zhang, X., Mao, Y., et al., 2000. Locally resonant sonic materials. Science 289, 1734–1736.

Monsivais, G., Otero, J.A., Calás, H., 2005. Surface and shear horizontal waves in piezoelectric composites. Phys. Rev. B 71, 064101.

Pang, Yu, Gao, Jin-Shan, Liu, Jin-Xi, 2014. SH wave propagation in magnetic–electric periodically layered plates. Ultrasonics 54, 1341–1349.

Pang, Yu, Liu, Jin-Xi, 2011. Reflection and transmission of plane waves at an imperfectly bonded interface between piezoelectric and piezomagnetic media. Eur. J. Mech. A/Solids 30, 731–740.

Pang, Yu, Liu, Jinxi, Wang, Yuesheng, Fang, Daining, 2008. Wave propagation in piezoelectric /piezomagnetic layered periodic composites. Acta Mech. Solida Sin 21 (6), 483–490.

Piliposyan, D., 2012. Shear surface waves at the interface of two magneto-electro-elastic media. Multidiscip. Model. Mater. Struct 8, 417–426.

Qian, Z., Jin, F., Kishimoto, K., Wang, Z., 2004. Effect of initial stress on the propagation behavior of SH-waves in multilayered piezoelectric composite structures. Sens. Actuators A 112, 368–375.

Qian, Zhenghua, Jin, Feng, Wang, Zikun, Kishimoto, Kikuo, 2004. Dispersion relations for SH-wave propagation in periodic piezoelectric composite layered structures. Int. J. Eng. Sci 42, 673–689.

Sigalas, M.M., Economou, E.N., 1992. Elastic and acoustic wave band structure. J. Sound Vib. 158 (2), 377–382.

Sun, Wei-Hai, Ju, Gui-Ling, Pan, Jing-Wen, Li, Yong-Dong, 2011. Effects of the imperfect interface and piezoelectric/piezomagnetic stiffening on the SH wave in a multiferroic composite. Ultrasonics 51, 831–838.

Suzuki, Toshio, Yu Paul, K.L., 1998. Complex elastic wave band structures in three-dimensional periodic elastic media. J. Mech. Phys Solids. 46 (1), 115–138.

Wang, X., Sudak, L.J., 2007. A piezoelectric screw dislocation interacting with an imperfect piezoelectric biomaterial interface. Int. J. Solids Struct 44, 3344–3358.

Wang, Yi-Ze, Li, Feng-Ming, Huang, Wen-Hu, Jiang, Xiaoai, Wang, Yue-Sheng, Kishimoto, Kikuo, 2008. Wave band gaps in two-dimensional piezoelectric/piezomagnetic phononic crystals. Int. J. Solids Struct 45, 4203–4210.

Wang, Yi-Ze, Li, Feng-Ming, Kishimoto, Kikuo, Wang, Yue-Sheng, Huang, Wen-Hu, 2010. Band gaps of elastic waves in three-dimensional piezoelectric phononic crystals with initial stress. Eur. J. Mech. A/Solids 29, 182–189.

Zheng, Min, Wei, Pei-Jun, 2009. Band gaps of elastic waves in 1-D phononic crystals with imperfect interfaces. Int. J. Min, Metall. Mater 16 (5), 608–614.